Data were acquired with a Nicolet lab computer. All electrochemistry was done under an atmosphere of purified argon.

THF was distilled immediately prior to use from sodium benzophenone. Propylene carbonate was vacuum-distilled by employing a commercial spinning-band distillation apparatus. Supporting electrolytes were purchased from Eastman Chemicals and dried in vacuo at 100 °C for at least 1 h immediately prior to use.

NMR data were obtained on a Varian XL-200 or Nicolet 360-MHz instrument. IR data were obtained on a Perkin-Elmer 283 spectrometer. THF was distilled from sodium benzophenone immediately prior to use. THF-d_8 was pot-to-pot distilled from sodium or P_2O_5 after at least five freeze–pump–thaw cycles to remove any O_2. Dioxane was freshly distilled from Na/K alloy immediately prior to use. All work was done under argon (dried and deoxygenated) with use of standard manifold techniques.

Preparation of I, XIII, and XIV. Naphthalene (9.44 g, 0.072 mol) and hexacarbonylchromium (8.80 g, 0.040 mol) were refluxed in a 36-mL mixture of dioxane/THF (6/1 by volume) for 6 days. The reaction was then filtered and the solvent removed under reduced pressure. Purification was accomplished by column chromatography on silica gel, employing hexane/diethyl ether as eluent. ^{1}H NMR and IR bands and melting points all agreed with literature values.[59-61,95]

Preparation of IV. I (0.264 g, 1.0 mmol) was dissolved in 1.0 mL of THF or THF-d_8, depending on the purpose of the experiment. This solution was then added to the Na/Hg amalgam prepared by adding 0.1 g of Na to 1 mL of Hg with stirring. The amalgam was prepared in the reaction flask. This mixture was allowed to react until the IR spectrum of I disappeared (approximately 0.25 h). The solution was filtered and used.

Preparation of II. (a) The sodium salt of II can be prepared by adding an equimolar amount of H_2O to the solution of IV as prepared above. Filtration, followed by removal of the solvent under vacuum, yields a purple solid, which has been characterized as II.

(b) II with tetraethylammonium as the counterion can be prepared by adding tetraethylammonium chloride to the solution prior to filtration. If this mixture is stirred for 2 h and then worked up as in (a), the Et_4N^+ salt of II is obtained.

Acknowledgment. We thank the National Science Foundation for support of this research (Grant CHE-8318335). We also wish to thank T. Albright for helpful discussions and R. Baker and T. Tulip for a preprint of their paper.

Contribution from the Chemistry Department,
The Ohio State University, Columbus, Ohio 43210

Inclusion Complexes Involving a Novel Ligand Superstructure: Dioxygen Adducts and Other Derivatives of Retro-Bridged Cyclidene Iron, Cobalt, and Nickel Complexes

James H. Cameron, Masaaki Kojima, Bohdan Korybut-Daszkiewicz, Bradley K. Coltrain, Thomas J. Meade, Nathaniel W. Alcock,† and Daryle H. Busch*

Received December 3, 1985

New iron(II) and cobalt(II) dioxygen carriers have been synthesized with a novel family of *retro-bridged* lacunar cyclidene ligands (structure V) by consecutive template reactions. NMR and ESR spectroscopy, electrochemistry, and equilibrium studies have been applied to the characterization of the new dioxygen carriers. The cobalt complexes unambiguously demonstrate steric control of dioxygen affinity while the iron(II) complexes exhibit both greater dioxygen affinities than previously reported iron(II) lacunar cyclidene complexes and surprisingly moderate sensitivity toward autoxidation. By combining the new retro-bridge with the previously known bridging reaction, both lacunar (structure VI) and vaulted (structure VII) *doubly bridged* cyclidene complexes of nickel(II) have been prepared. The X-ray crystal structure determination of [Ni{$(CH_2)_8(CH_2pipz)_2$(3,6-dur)[16]cyclidene}]$(PF_6)_2 \cdot CH_3CN$ is reported and the results applied to the understanding of the chemistry of the unusual compound: orthorhombic, space group $Pna2_1$; cell parameters a = 18.863 (4) Å, b = 19.822 (3) Å, c = 13.761 Å, Z = 4.

Introduction

Inclusion chemistry is among the most promising contemporaneous areas for applying molecular design to the investigation of chemical relationships involving the association of independent chemical entities. The classic case of metal coordination templates was addressed long ago by one of us,[1] while Cram has clearly delineated the host–guest relationships for the case where a guest is included within the cylindrical cavity of a macrocyclic host.[2] Lehn and others have considered more complex mixed cyclic structures designed to include two or more guests or more than one functional moiety in a single guest.[3] There is a parallel between this molecular design and the so-called compartmental ligands, defined by Fenton,[4] which coordinate two, or more, metal ions in well-defined coordination sites. The first such ligand was probably that reported by Travis and Busch.[5] Subsequently, we have departed from these single-function host or ligand molecules and designed ligands having sites for accommodating two or three different classes of included species.[6-9]

Lacunar cyclidene complexes (structure I) were designed to provide new families of dioxygen carriers.[10] The ligands are

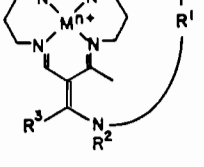

I

bicyclic structures in which one cycle accommodates the metal ion (cobalt(II) or iron(II)) while the second ring provides a

* To whom correspondence should be addressed.
† Department of Chemistry, University of Warwick, Coventry CV4 7AL, England.

(1) Thompson, M. C.; Busch, D. H. *J. Am. Chem. Soc.* **1964**, *86*, 3651.
(2) Cram, D. J.; Kameda, T.; Helgeson, R. C.; Brown, S. B.; Knobler, C. B.; Maverick, E.; Trueblood, K. N. *J. Am. Chem. Soc.* **1985**, *107*, 3645.
(3) (a) Lehn, J. M. *Acc. Chem. Res.* **1978**, *11*, 49. (b) Motekaitis, R. J.; Martell, A. E.; Lehn, J. M.; Watanabe, E. *Inorg. Chem.* **1982**, *21*, 4253.
(4) (a) Fenton, E. E.; Gayda, S. E. *J. Chem. Soc., Chem. Commun.* **1974**, 960. (b) Fenton, D. E.; Gayda, S. E. *J. Chem. Soc., Dalton Trans.* **1977**, 2095.
(5) Busch, D. H.; Travis, K. *J. Chem. Soc. D* **1970**, 1041.
(6) Meade, T. J.; Busch, D. H. *Prog. Inorg. Chem.* **1985**, *33*, 59.
(7) Takeuchi, K. J.; Alcock, N.; Busch, D. H. *J. Am. Chem. Soc.* **1981**, *103*, 2421.
(8) Takeuchi, K. J.; Alcock, N.; Busch, D. H. *J. Am. Chem. Soc.* **1983**, *105*, 4261.
(9) Takeuchi, K. J.; Busch, D. H. *J. Am. Chem. Soc.* **1983**, *105*, 6812.

0020-1669/87/1326-0427$01.50/0

permanent void within which the dioxygen molecule or some other small ligand may be coordinated to the metal ion. While novel, the lacunar structure is not a unique example of its structural type; a variety of examples have been reported among superstructured porphyrin ligands.

The *vaulted* cyclidene ligands (structure II) are, however, unique because of their ability to *occlude* three different kinds of chemical species simultaneously.[7-9] The ligand molecules are

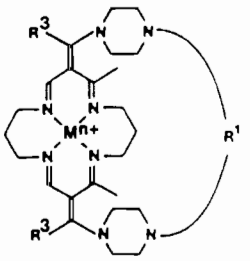

II

macrobicycles so designed that they may accommodate a metal ion within one macrocycle and both a small ligand molecule and an organic *guest* molecule within the extensive void associated with the second macrocyclic component.[9]

Our earlier studies have shown that the positioning of the group R^1 above the parent cyclidene macrocycle creates permanent voids within both *lacunar* and *vaulted* cyclidene complexes. This is illustrated in the corresponding three-dimensional sketches (structures III and IV). The lacunar complexes of cobalt are

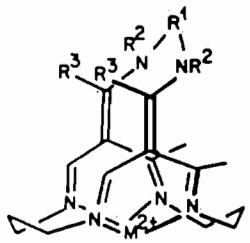

III

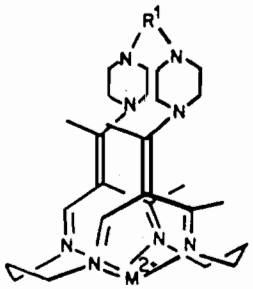

IV

exceptional in several ways: (a) the dioxygen affinity (K_{O_2}) is controlled by the void dimensions, among other factors, and may range over at least 5 orders of magnitude; (b) some examples exhibit unusually large dioxygen affinities, surpassing even those of most iron(II) dioxygen carriers; (c) the rates of autoxidation of the cobalt(II) dioxygen carriers are unusually slow, especially in protic solvents.[11]

The lacunar iron(II) complexes are even more remarkable.[12] Except for the porphyrins, the lacunar cyclidene complexes of iron(II) are the only known extensive family of dioxygen carriers based on iron. Further, certain of these are fully functional under ambient conditions. The *vaulted* cyclidene complexes were developed with the expectation that they would form ternary complexes containing the metal–cyclidene complex, bound dioxygen, and a bound substrate molecule.[12] These species are models for the ternary complexes of such oxygenase enzymes as cytochrome P450 and are prototypes for synthetic catalysts designed to mimic those enzymes.

In those compounds reported in prevous studies, the crucial second ring (in addition to the cyclidene ring) involved the R^1 groups (structures I–IV). Here we report the design, synthesis, and behavior of related compounds in which the bridging ring closure occurs at the R^3 position (structure V). The bridge in

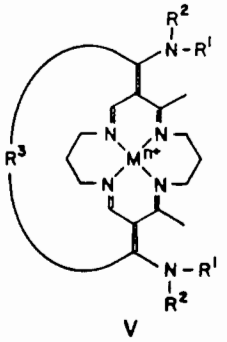

V

these systems is a polymethylene linkage, which, in contrast to those in structures I and II, contains no nitrogen atoms. Cobalt(II) and iron(II) derivatives have been prepared, and their dioxygen-binding reactions have been investigated.

In a further extension of the molecular design, we have synthesized new families of tricyclic, doubly bridged structures by combining the two bridging processes. Examples with this tricyclic structure are reported for both the lacunar (structure VI) and vaulted (structure VII) complexes. In common with the case for

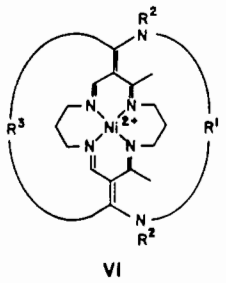

VI

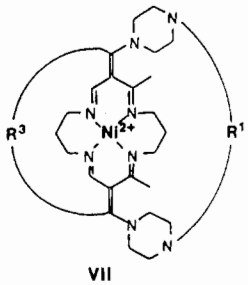

VII

the cyclidene derivatives reported earlier, the ligands are synthesized by template reactions on nickel(II).

Results and Discussion

Synthesis and Properties of the Retro-Bridged Nickel(II) Complexes. Scheme I outlines the procedures used to introduce the R^3 bridging group into the cyclidene structure IV. The starting material is the nickel(II) complex of the well-known 16-membered macrocyclic ligand first reported by Jäger.[13] The first step is deacylation, yielding a protonated cationic complex. Deprotonation to form the neutral complex is then followed by the ring closure reaction using the diacid chloride appropriate for the desired polymethylene chain as bridging group. Chain lengths varying from five to eight carbon atoms were used in this procedure. The intermediates formed in this way are simple bicyclic variants of the Jager complexes.

The bicyclic complexes are converted to cyclidene complexes

(10) Schammel, W. P.; Mertes, K. S. B.; Christoph, G. G.; Busch, D. H. *J. Am. Chem. Soc.* **1979**, *101*, 1622.
(11) (a) Stevens, J. C.; Jackson, P. J.; Schammel, W. P.; Christoph, G. G.; Busch, D. H. *J. Am. Chem. Soc.* **1980**, *102*, 3283. (b) Stevens, J. C.; Busch, D. H. *J. Am. Chem. Soc.* **1980**, *102*, 3285.
(12) (a) Herron, N.; Busch, D. H. *J. Am. Chem. Soc.* **1981**, *103*, 1236. (b) Herron, N.; Cameron, J. H.; Neer, G. L.; Busch, D. H. *J. Am. Chem. Soc.* **1983**, *105*, 298.
(13) Jäger, E. *Z. Chem.* **1968**, *8*, 392.

Scheme I

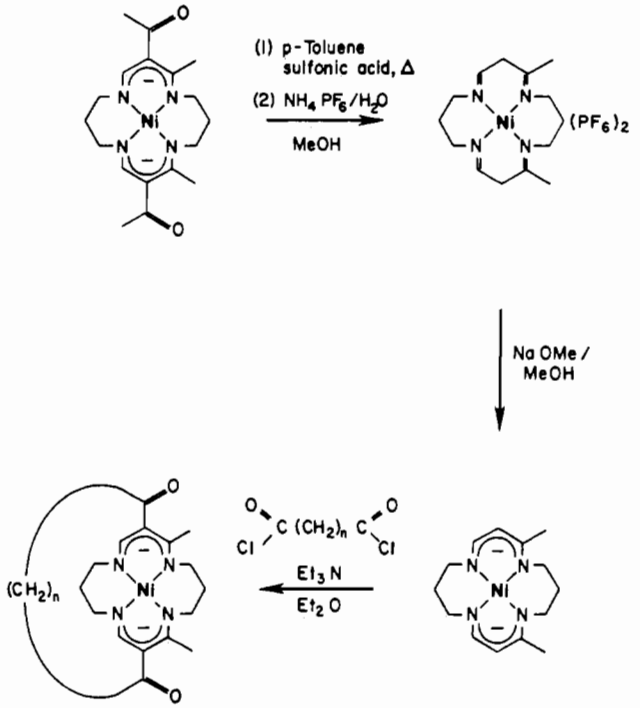

by the same sequence of reactions used to produce the previously reported R^1-bridged species (Scheme II).[14-16] Table I presents the results of elemental analyses on the new compounds. The complexes can be divided into two groups. The first comprise *retro-bridged* lacunar cyclidene complexes (structure V) with the R^3 bridge ranging from pentamethylene to octamethylene for the case where the nitrogen substituent is $-NMe_2$, from hexamethylene to octamethylene with $-NHMe$, and a heptamethylene-bridged example with $-NH(n\text{-Pr})$. The ligands of the second group are doubly bridged cyclidenes, and examples include lacunar nickel(II) complexes (structure VII) having the following combinations of bridging groups: $R^1 = (CH_2)_6$ for $R^3 = (CH_2)_n$, $n = 6$–8; $R^1 = (CH_2)_7$ for $R^3 = (CH_2)_8$; $R^1 = m$-xylylene for $R^3 = (CH_2)_n$, $n = 7,8$. In addition, the doubly bridged vaulted complex has been synthesized for $R^3 = (CH_2)_8$ and with the vault composed of piperazine risers and a durylene roof (structure VII). The crystal structure of this complex confirms the structures of these families of R^3-bridged complexes (vide infra).

The ^{13}C NMR chemical shift data for eight nickel(II) complexes having structures V and VI are listed in Table II. The shifts were assigned with the aid of off-resonance decoupling, to determine the number of hydrogen atoms directly bonded to each carbon atom, and by comparison with spectra of similar complexes.[15,16] The spectra of all the complexes exhibit the resonances expected for the carbon atoms of the parent macrocycle,[15,16] and these need not be considered further. The spectra also show multiple resonances in the methylene region, and the assignment of these peaks to specific carbon atoms is generally difficult although some salient features can be identified.

Perhaps the most significant feature occurs for the retro-bridged complexes of structure V having $R^1 = R^2 = Me$. It is a methyl carbon resonance at 45.1–44.5 ppm. The resonance is sharp for the shorter polymethylene chain derivatives; however, as the bridge length increases, this spectral feature broadens until it is very broad

Scheme II

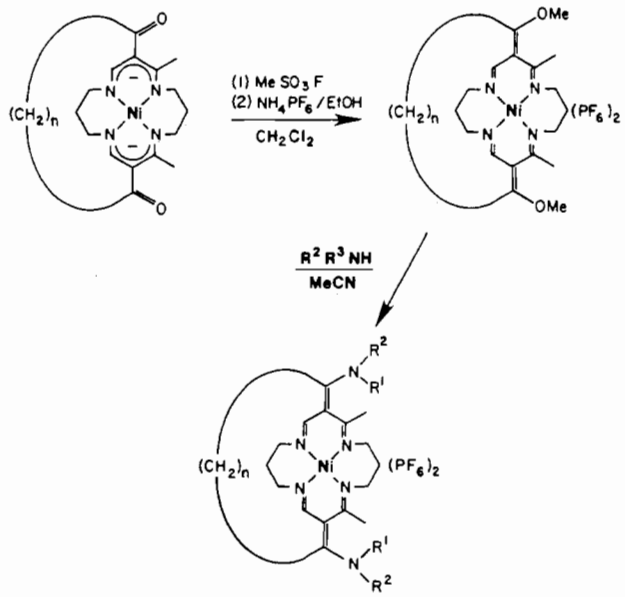

and indistinct at $R^3 = (CH_2)_8$. This is attributed to changes in the rate of rotation about the C–N bond and, hence, interconversion of R^1 and R^2; the rate decreases as the length of the bridging chain increases. Cooling a solution of the heptamethylene-bridged complex to 248 K resulted in the splitting of this resonance into two signals separated by 5.6 ppm. Under these conditions, the rate of rotation is sufficiently slow for distinct resonances to be observed for each of the methyl groups. This kind of intramolecular motion is not evident for the complexes with $R^2 = H$.

The change in the rate of rotation about the C–N bond can be rationalized by considering the resonance forms that contribute to the overall electronic structure of the ligand in a retro-bridged cyclidene complex. Crystal structures of R^1-bridged complexes imply considerable delocalization, with the C–N bond having appreciable double-bond character (structure VIII). The greater

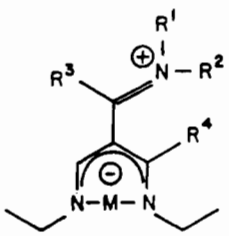

VIII

the contribution of VIII to the overall structure, the slower will be the rotation about the C–N bond. The results for the R^3-bridged complexes suggest that structure VIII is relatively unimportant for the pentamethylene derivative but that it becomes increasingly important for longer bridging units. The charge displacement in structure VIII also suggests that the electron density at the metal atom might increase in parallel with the contribution due to that structure, i.e., with increasing bridge length. This is discussed further below in conjunction with the electrochemical properties of these complexes.

A variation, concurrent with that just described, is observed for NMR features associated with the bridging methylene groups. The pentamethylene derivative shows a sharp methylene resonance at 38.8 ppm in its room-temperature spectrum. A similar resonance for the hexamethylene derivative is broadened and shifted to 36.2 ppm. For the heptamethylene and octamethylene species, the resonance is very broad and occurs at the same chemical shift as the resonances for the other methylene groups (~30.2 and 28.0

(14) Olszanski, D. J.; Stevens, J. C.; Schammel, W. P.; Kojima, M.; Herron, N.; Zimmer, L. L.; Holter, K. A.; Mocak, J.; Busch, D. H. *J. Am. Chem. Soc.* **1981**, *103*, 1472.

(15) (a) Busch, D. H.; Jackels, S. C.; Callahan, R. W.; Grzybowski, J. J.; Zimmer, L. L.; Kojima, M.; Olszanaski, D. J.; Schammel, W. P. *Inorg. Chem.* **1981**, *20*, 2834. (b) Busch, D. H.; Zimmer, L. L.; Grzybowski, J. J.; Olszanski, D. J.; Jackels, S. S.; Callahan, R. W.; Christoph, G. G. *Proc. Natl. Acad. Sci. U.S.A.* **1981**, *78*, 5919.

(16) Herron, N.; Zimmer, L. L.; Grzybowski, J. J.; Olszanski, D. J.; Jackels, S. C.; Callahan, R. W.; Cameron, J. H.; Christoph, G. G.; Busch, D. H. *J. Am. Chem. Soc.* **1983**, *105*, 6585.

(17) Goldsby, K. A.; Meade, T. J.; Kojima, M.; Busch, D. H. *Inorg. Chem.* **1985**, *24*, 2588.

Table I. Analytical Data for the Nickel(II) Complexes of the R^3-Bridged Lacunar Ligands (Structures V and VI, PF_6^- Salts)

			anal., %					
			calcd			obsd		
n[a]	R^2	R^1	C	H	N	C	H	N
5	Me	Me	38.73	5.46	10.84	38.68	5.63	10.93
6[b]	H	Me	38.92	5.40	12.22	39.18	5.53	12.2
6[b]	Me	Me	40.50	5.70	11.81	40.49	5.93	11.86
6	H	2 R^1 = $(CH_2)_6$	41.25	5.69	10.31	41.23	6.19	10.41
7	H	Me	38.71	5.46	10.84	38.79	5.50	10.82
7	Me	Me	40.37	5.77	10.46	40.21	5.82	10.37
7	H	*n*-Pr	41.90	6.06	10.11	41.86	6.05	10.16
7	H	2 R^1 = $(CH_2)_6$	42.00	5.83	10.13	41.91	5.86	10.00
7	H	2 R^1 = *m*-xylyl	43.84	5.22	9.89	44.19	4.78	9.90
8	H	Me	39.56	5.62	10.65	39.44	5.70	10.50
8	Me	Me	41.15	5.92	10.28	41.08	5.98	10.10
8	H	2 R^1 = $(CH_2)_6$	42.72	5.98	9.96	42.99	6.00	9.91
8[c]	H	2 R^1 = *m*-xylyl	44.90	5.76	9.24	45.31	5.87	9.60
8	H	2 R^1 = $(CH_2)_7$	43.42	6.11	9.80	43.62	6.24	9.80

[a] For the $(CH_2)_n$ bridge. [b] Contains 1 mol of CH_3CN. [c] Contains 1 mol of C_2H_5OH.

Table II. ^{13}C NMR Data for R^3-Bridged Nickel(II) Complexes[a] Having Structures V and VI

R^3	R^2	R^1	chem shifts, ppm
$(CH_2)_5$	Me	Me	178.7, 168.4, 157.2, 111.6, 55.0, 51.2, 45.1, 38.8, 31.9, 30.5, 30.2, 22.7
$(CH_2)_6$	Me	Me	167.7, 157.3, 110.0, 55.3, 50.6, 44.9, 36.2,[b] 30.9, 30.3, 28.5, 21.8
$(CH_2)_7$	Me	Me	170.4, 161.7, 112.7, 55.9, 50.6, 44.5, 31.3, 30.2, 29.8, 29.3, 29.1, 21.8
$(CH_2)_8$	Me	Me	172.4, 170.7, 161.7, 56.2, 50.5, 31.5, 29.8, 29.4, 29.0, 28.3, 26.9, 21.6
$(CH_2)_7$	*n*-Pr	H	169.0, 168.9, 161.5, 112.6, 55.8, 50.8, 47.2,[b] 31.4, 29.9, 29.5, 29.1, 28.6, 27.0,[b] 23.7, 21.1, 11.5
$(CH_2)_8$	H	$(CH_2)_7$	169.8, 169.2, 161.1, 114.0, 56.5, 51.4, 45.7, 31.8, 30.3, 30.0, 29.2, 28.8, 27.6, 27.0, 21.1
$(CH_2)_8$	Me	$(CH_2)_6$	163.5, 159.3, 58.1, 57.7, 55.0, 52.4, 49.9, 38.5, 31.5, 30.1, 29.5, 28.8, 28.2, 27.8, 22.4, 20.0
$(CH_2)_7$	H	$(CH_2)_6$	169.0, 168.9, 161.5, 112.7, 55.8, 50.8, 45.3, 31.4, 30.1, 30.0, 29.5, 29.1, 28.8, 28.7, 26.9, 21.1

[a] CD_3CN solution, relative to Me_4Si. [b] Broad.

Table III. Electrochemical Data for the R^3-Bridged Nickel(II) Complexes[a]

			oxidn				redn			
R^3	R^1	R^2	$E_{1/2}$, V	Δ_1,[b] mV	E_p, V	Δ_2,[b] mV	$E_{1/2}$, V	Δ_1, mV	E_p, V	Δ_2, mV
$(CH_2)_6$	CH_3	H	0.89	90	0.92	70	−1.94	...	−1.98	
			1.21	110	1.21[c]	...			−2.25[d]	
$(CH_2)_7$	CH_3	H	0.89	70	0.92	70	−1.84	80	−1.95	...
			1.17	80	1.21	80	−2.1[e]			
$(CH_2)_8$	CH_3	H	0.92	60	0.95	80	−1.97[f]	...	−1.88[f]	...
			1.22	80	1.28	...				
$(CH_2)_7$	*n*-Pr	H	0.89	70	0.92	70	*f*		−1.78	
			1.17	80	1.20	80	−2.1[e]		...	
$(CH_2)_8$	CH_3	CH_3	*f*		*f*				−1.73	...
							−1.85	80	−1.88	...
									−2.27	...
									−2.45	...
$(CH_2)_7$	CH_3	CH_3	0.68		0.72				−1.19	
			f		1.17		−1.88[h]			
			f		1.32				−2.25	
									−2.51	
$(CH_2)_6$	CH_3	CH_3	0.60	70	0.63	60	*f*		−1.29	
			1.00	80	1.03				−2.20	
									−2.48	
$(CH_2)_5$	CH_3	CH_3	0.67	70	0.70	60	−1.91	60	−1.94	
			1.00	70	1.03	60	*d*		−2.15	
									−2.50	
$(CH_2)_6$	2 R^1 = $(CH_2)_6$	H	0.9[f]		*f*		*f*		*f*	
$(CH_2)_7$	2 R^1 = $(CH_2)_6$	H	0.96	*g*	0.99[g]	...	−1.89	100	−1.93	
			1.17	*g*	1.19[g]	...			−2.17	
$(CH_2)_8$	2 R^1 = $(CH_2)_6$	H	1.06	140	1.12	...	−1.88			
					1.52	...			−2.15	
									−2.4	
$(CH_2)_8$	2 R^1 = $(CH_2)_7$	H			0.98	115				
$(CH_2)_7$	2 R^1 = *m*-xylyl	H	*f*		1.03				−1.05	
					1.20		−1.75	110	−1.89	
									−2.24	

[a] Conditions: in CH_3CN solution, 0.1 N $(n\text{-}Bu)_4NBF_4$ supporting electrolyte, $Ag/AgNO_3$ (0.1 M) reference electrode. [b] $\Delta_1 = |E_{3/4} - E_{1/4}|$ from RPE; $\Delta 2 = |E_p - E_{p/2}|$ from CV. [c] Counterpeak in CV ill-defined. [d] No corresponding wave in RPE. [e] No corresponding CV peak. [f] Irregular or ill-defined wave. [g] Peaks are broad. [h] Only one RPE peak seen for reduction.

ppm, respectively). This resonance is assigned to the methylene group adjacent to the bridgehead carbon atom, and its broadening is associated with the slowing of the rate of rotation of the $-N(Me)_2$ group.

Table IV. Crystal Data for [Ni{$(CH_2)_8(CH_2pipz)_2$(3,6-dur)[16]cyclidene}]$(PF_6)_2 \cdot CH_3CN$ (Structure VII)

formula	$NiC_{44}H_{68}N_8P_2F_{12} \cdot CH_3CN$
fw	1098.77
cell parameters	
a, Å	18.863 (4)
b, Å	19.822 (3)
c, Å	13.761 (3)
V, Å^3	5145 (2)
syst, space group	orthorhombic, $Pna2_1$
Z	4
$F(000)$	2247
2θ range, deg	2.0–50.0
ρ_{calcd}, g cm^{-3}	1.418
ρ_{obsd}, g cm^{-3}	1.39 (1)
cryst dimens, mm	0.60 × 0.31 × 0.26
T, K	290
radiation	Mo K$\bar{\alpha}$ (graphite-monochromated)
λ, Å	0.710 69
μ, cm^{-1}	5.21
octants collected	$+h,+k,+l$
no. of indep reflecns	3794
no. of reflecns with $I \geq 2.5\sigma(I)$	2709
final R	0.055
R'_w	0.058

The results of electrochemical studies on the nickel(II) complexes having structures V and VI are summarized in Table III, and attention is directed to the first oxidation process, which has been assigned to the Ni^{II}/Ni^{III} couple. The oxidation and reduction waves assigned to the ligands are included, but these will not be discussed in detail. It should be mentioned that the ligand processes appear to be very similar for a variety of ligands having different superstructures. The metal-centered processes range from quasi-reversible to irreversible, and the values of both their half-wave potentials, from RPE experiments, and their peak potentials, from CV measurements, are reported.

The value for the half-wave potential for the Ni^{II}/Ni^{III} couple is about 0.90 V and is independent of the length of the bridge for retro-bridged nickel(II) complexes (structure V) having R^2 = H and R^1 = Me. This value is very similar to those found for complexes of structure I, which have an N–H substituent. Indeed, $E_{1/2}$ = 0.90 V for the R^1-bridged complex having $R^1 = (CH_2)_6$, R^2 = Me, and R^3 = H.

Not surprisingly, when the N–H group is replaced by N–Me, the potential shifts in the negative direction for the retro-bridged complex. For the four complexes of structure V with $R^1 = R^2$ = Me, the potential falls in the range 0.60 to ~0.70 V vs. Ag/Ag^+ in acetonitrile solution; however, the electrochemical behavior is not well-defined for the longer chain derivatives. Although the potential ranges over 100 mV, it apparently does not depend on bridge length. Comparison with data for complexes of structure I[14] having N–Me substituents suggests that the new retro-bridged complexes (structure V) are ~100 mV easier to oxidize. For example, the complex I with $R^1 = (CH_2)_6$ and $R^2 = R^3$ = Me has $E_{1/2}$ = 0.78 V.

Recalling the bridge length dependence of the rate of rotation of the $-N(Me)_2$ group and the attendant prediction about the importance of resonance structure VIII, one might have expected the Ni^{II}/Ni^{III} couple to shift with the R^3 bridge length. However, we have observed previously that the lengths of R^1 bridges affect certain NMR properties that may be associated with the importance of resonance structure VIII but that this does not affect the potential of the Ni^{II}/Ni^{III} couple and therefore has little effect on the electron density at the metal ion.[17] It is gratifying to see this congruent behavior in cyclidene complexes differing so widely in structure.

The doubly bridged nickel(II) complexes (structure VI) generally give poorly definable electrochemical results, and no significant correlations can be made. The Ni^{II}/Ni^{III} couples of such complexes appear in the range from 0.90 to 1.06 V. All of the complexes have R^1 = H, so this is within the range expected on the basis of the singly bridged complexes.

Table V. Positional Parameters for [Ni{$(CH_2)_8(CH_2pipz)_2$(3,6-dur)[16]cyclidene}]$(PF_6)_2 \cdot CH_3CN$ (Structure VII)

	x	y	z	U, Å^2
Ni	0.1883 (1)	0.0755 (1)	0.5000	0.039 (1)
P(1)	0.5084 (1)	0.3926 (1)	0.1809 (2)	0.054 (1)
P(2)	0.0162 (2)	0.7303 (2)	0.2037 (2)	0.068 (1)
F(11)	0.5082 (4)	0.3128 (3)	0.1889 (6)	0.113 (3)
F(12)	0.5550 (4)	0.3903 (4)	0.0881 (5)	0.103 (3)
F(13)	0.4389 (4)	0.3890 (4)	0.1170 (5)	0.107 (3)
F(14)	0.5772 (3)	0.3950 (4)	0.2474 (5)	0.086 (3)
F(15)	0.4605 (3)	0.3944 (3)	0.2767 (4)	0.072 (2)
F(16)	0.5087 (3)	0.4716 (2)	0.1769 (5)	0.083 (2)
F(21)	−0.0021 (4)	0.8060 (3)	0.2073 (8)	0.138 (4)
F(22)	−0.0248 (6)	0.7167 (5)	0.2994 (7)	0.180 (6)
F(23)	0.0353 (5)	0.6541 (4)	0.2000 (9)	0.146 (5)
F(24)	0.0539 (4)	0.7429 (5)	0.1053 (6)	0.143 (4)
F(25)	−0.0557 (4)	0.7200 (4)	0.1475 (7)	0.146 (4)
F(26)	0.0875 (4)	0.7415 (4)	0.2586 (6)	0.131 (3)
N(1)	0.2395 (4)	−0.0010 (4)	0.5430 (5)	0.049 (3)
N(2)	0.2568 (4)	0.1339 (4)	0.5551 (5)	0.046 (3)
N(3)	0.1402 (3)	0.1519 (3)	0.4555 (5)	0.038 (2)
N(4)	0.1206 (3)	0.0160 (3)	0.4480 (5)	0.037 (2)
N(5)	0.2136 (4)	−0.0995 (4)	0.2269 (5)	0.047 (3)
N(6)	0.1941 (4)	−0.0850 (3)	0.0212 (5)	0.055 (3)
N(7)	0.2792 (4)	0.2246 (3)	0.0462 (5)	0.048 (3)
N(8)	0.2714 (4)	0.2457 (3)	0.2531 (4)	0.041 (2)
C(1)	0.2519 (5)	−0.0499 (5)	0.4827 (7)	0.051 (4)
C(2)	0.2118 (5)	−0.0585 (4)	0.3940 (8)	0.038 (4)
C(3)	0.1376 (5)	−0.0385 (5)	0.4011 (7)	0.033 (3)
C(4)	0.0804 (4)	−0.0876 (4)	0.3699 (7)	0.047 (3)
C(5)	0.2427 (5)	−0.0937 (4)	0.3162 (7)	0.044 (3)
C(6)	0.2299 (5)	−0.1549 (4)	0.1593 (7)	0.060 (4)
C(7)	0.2497 (6)	−0.1260 (5)	0.0603 (7)	0.068 (4)
C(8)	0.1792 (6)	−0.0278 (5)	0.0856 (8)	0.057 (4)
C(9)	0.1587 (5)	−0.0552 (5)	0.1861 (7)	0.057 (4)
C(10)	0.2025 (2)	−0.0656 (2)	−0.0825 (3)	0.067 (4)
C(11)	0.2361	0.0031	−0.1026	0.044 (3)
C(12)	0.1911	0.0584	−0.1143	0.048 (3)
C(13)	0.2176	0.1237	−0.1047	0.049 (3)
C(14)	0.2891	0.1338	−0.0834	0.052 (4)
C(15)	0.3341	0.0786	−0.0717	0.055 (4)
C(16)	0.3076	0.0132	−0.0813	0.052 (4)
C(17)	0.1138 (5)	0.0521 (6)	−0.1465 (10)	0.084 (5)
C(18)	0.1723 (6)	0.1860 (5)	−0.1237 (9)	0.086 (5)
C(19)	0.4110 (6)	0.0909 (7)	−0.0538 (12)	0.098 (7)
C(20)	0.3607 (6)	−0.0459 (5)	−0.0894 (10)	0.092 (5)
C(21)	0.3115 (6)	−0.2025 (5)	−0.0445 (8)	0.077 (4)
C(22)	0.3267 (5)	0.2725 (5)	0.0956 (7)	0.044 (4)
C(23)	0.2944 (5)	0.2994 (5)	0.1875 (7)	0.050 (4)
C(24)	0.2238 (5)	0.1974 (5)	0.2028 (7)	0.046 (4)
C(25)	0.2606 (5)	0.1693 (4)	0.1147 (7)	0.049 (4)
C(26)	0.2916 (5)	0.2377 (4)	0.3467 (7)	0.037 (3)
C(27)	0.2506 (5)	0.2044 (5)	0.4143 (7)	0.038 (3)
C(28)	0.2813 (5)	0.1821 (4)	0.5050 (8)	0.041 (3)
C(29)	0.1734 (5)	0.2001 (4)	0.4109 (7)	0.037 (3)
C(30)	0.1320 (5)	0.2584 (4)	0.3693 (8)	0.046 (4)
C(31)	0.0635 (4)	0.1566 (4)	0.4717 (7)	0.046 (3)
C(32)	0.0363 (5)	0.0957 (5)	0.5225 (8)	0.051 (4)
C(33)	0.0448 (4)	0.0298 (5)	0.4664 (7)	0.041 (3)
C(34)	0.2881 (6)	0.1227 (5)	0.6523 (8)	0.060 (4)
C(35)	0.3251 (6)	0.0539 (5)	0.6545 (8)	0.065 (4)
C(36)	0.2735 (5)	−0.0055 (5)	0.6388 (8)	0.070 (3)
C(37)	0.3678 (5)	0.2590 (5)	0.3698 (8)	0.048 (3)
C(38)	0.4218 (7)	0.2052 (7)	0.3594 (10)	0.090 (4)
C(391)	0.4060 (10)	0.1398 (10)	0.3062 (17)	0.084 (6)
C(392)	0.4173 (21)	0.1449 (19)	0.3833 (32)	0.091 (13)
C(40)	0.4597 (9)	0.0880 (7)	0.3198 (15)	0.144 (6)
C(41)	0.4407 (9)	0.0285 (8)	0.2606 (13)	0.120 (6)
C(421)	0.3745 (12)	−0.0204 (12)	0.2539 (20)	0.119 (8)
C(422)	0.3855 (12)	−0.0125 (12)	0.3205 (18)	0.015 (7)
C(431)	0.3759 (9)	−0.0631 (9)	0.3336 (15)	0.083 (6)
C(432)	0.3702 (17)	−0.0832 (16)	0.2771 (26)	0.041 (10)
C(44)	0.3170 (6)	−0.1221 (6)	0.3277 (9)	0.065 (3)
N(51)	0.0458 (9)	0.2814 (8)	0.0191 (14)	0.194 (6)
C(51)	0.0805 (11)	0.3272 (10)	0.0741 (17)	0.154 (8)
C(52)	0.0968 (11)	0.3620 (11)	0.1318 (20)	0.178 (8)

In order to form complexes with metal ions other than the templating nickel(II) ion, it is necessary to remove the ligand and

Table VI. Bond Lengths (Å) for $[Ni\{(CH_2)_8(CH_2pipz)_2(3,6\text{-dur})[16]cyclidene\}](PF_6)_2 \cdot CH_3CN$ (Structure VII)

	(a) Coordination Sphere		
Ni–N(1)	1.893 (7)	Ni–N(3)	1.869 (6)
Ni–N(2)	1.893 (7)	Ni–N(4)	1.880 (6)
	(b) Ligand		
N(1)–C(1)	1.30 (1)	N(1)–C(36)	1.47 (1)
N(2)–C(28)	1.27 (1)	N(2)–C(34)	1.48 (1)
N(3)–C(29)	1.30 (1)	N(3)–C(31)	1.47 (1)
N(4)–C(3)	1.30 (1)	N(4)–C(33)	1.48 (1)
N(5)–C(5)	1.35 (1)	N(5)–C(6)	1.47 (1)
N(5)–C(9)	1.47 (1)	N(6)–C(7)	1.43 (1)
N(6)–C(8)	1.47 (1)	N(6)–C(10)	1.49 (1)
N(7)–C(21)	1.46 (1)	N(7)–C(22)	1.47 (1)
N(7)–C(25)	1.49 (1)	N(8)–C(23)	1.46 (1)
N(8)–C(24)	1.48 (1)	N(8)–C(26)	1.35 (1)
C(1)–C(2)	1.45 (2)	C(2)–C(3)	1.46 (1)
C(2)–C(5)	1.41 (1)	C(3)–C(4)	1.52 (1)
C(5)–C(44)	1.52 (1)	C(6)–C(7)	1.53 (1)
C(8)–C(9)	1.54 (1)	C(10)–C(11)	1.53
C(11)–C(12)	1.40 (1)	C(11)–C(16)	1.40
C(12)–C(13)	1.40	C(12)–C(17)	1.53 (1)
C(13)–C(14)	1.40	C(13)–C(18)	1.52 (1)
C(14)–C(15)	1.40	C(14)–C(21)	1.52 (1)
C(15)–C(16)	1.40	C(15)–C(19)	1.49 (1)
C(16)–C(20)	1.55 (1)	C(22)–C(23)	1.50 (1)
C(24)–C(25)	1.50 (1)	C(26)–C(27)	1.38 (1)
C(26)–C(37)	1.53 (1)	C(27)–C(28)	1.45 (2)
C(27)–C(29)	1.46 (1)	C(29)–C(30)	1.51 (1)
C(31)–C(32)	1.49 (1)	C(32)–C(33)	1.53 (1)
C(34)–C(35)	1.53 (2)	C(35)–C(36)	1.54 (2)
C(37)–C(38)	1.48 (2)	C(38)–C(391)	1.52 (2)
C(391)–C(40)	1.46 (2)	C(392)–C(40)	1.64 (4)
C(40)–C(41)	1.48 (2)	C(41)–C(421)	1.58 (3)
C(41)–C(422)	1.56 (3)	C(422)–C(432)	1.55 (4)
C(421)–C(431)	1.39 (3)	C(431)–C(44)	1.62 (2)
C(432)–C(44)	1.44 (3)		
	(c) PF_6^- Anions		
P(1)–F(11)	1.58 (1)	P(1)–F(12)	1.55 (1)
P(1)–F(13)	1.58 (1)	P(1)–F(14)	1.59 (1)
P(1)–F(15)	1.60 (1)	P(1)–F(16)	1.57 (1)
P(2)–F(21)	1.54 (1)	P(2)–F(22)	1.55 (1)
P(2)–F(23)	1.55 (1)	P(2)–F(24)	1.55 (1)
P(2)–F(25)	1.57 (1)	P(2)–F(26)	1.56 (1)
	(d) Solvent Acetonitrile		
C(51)–C(52)	1.10 (3)	N(51)–C(51)	1.35 (3)

Table VII. Bond Angles (deg) for $[Ni\{(CH_2)_8(CH_2pipz)_2(3,6\text{-dur})[16]cyclidene\}](PF_6)_2 \cdot CH_3CN$ (Structure VII)

	(a) Coordination Sphere		
N(1)–Ni–N(2)	90.9 (3)	N(1)–Ni–N(4)	87.9 (3)
N(2)–Ni–N(3)	88.1 (3)	N(3)–Ni–N(4)	93.1 (3)
	(b) Ligand		
Ni–N(1)–C(1)	119 (1)	Ni–N(1)–C(36)	124 (1)
C(1)–N(1)–C(36)	117 (1)	Ni–N(2)–C(28)	120 (1)
Ni–N(2)–C(34)	123 (1)	C(28)–N(2)–C(34)	117 (1)
Ni–N(3)–C(29)	121 (1)	Ni–N(3)–C(31)	119 (1)
C(29)–N(3)–C(31)	120 (1)	Ni–N(4)–C(3)	122 (1)
Ni–N(4)–C(33)	118 (1)	C(3)–N(4)–C(33)	119 (1)
C(5)–N(5)–C(6)	124 (1)	C(5)–N(5)–C(9)	126 (1)
C(6)–N(5)–C(9)	111 (1)	C(7)–N(6)–C(8)	111 (1)
C(7)–N(6)–C(10)	115 (1)	C(8)–N(6)–C(10)	114 (1)
C(21)–N(7)–C(22)	110 (1)	C(21)–N(7)–C(25)	115 (1)
C(22)–N(7)–C(25)	109 (1)	C(23)–N(8)–C(24)	111 (1)
C(23)–N(8)–C(26)	126 (1)	C(24)–N(8)–C(26)	123 (1)
N(1)–C(1)–C(2)	122 (1)	C(1)–C(2)–C(3)	114 (1)
C(1)–C(2)–C(5)	119 (1)	C(3)–C(2)–C(5)	126 (1)
N(4)–C(3)–C(2)	120 (1)	N(4)–C(3)–C(4)	120 (1)
C(2)–C(3)–C(4)	119 (1)	N(5)–C(5)–C(2)	125 (1)
N(5)–C(5)–C(44)	116 (1)	C(2)–C(5)–C(44)	119 (1)
N(5)–C(6)–C(7)	110 (1)	N(6)–C(7)–C(6)	112 (1)
N(6)–C(8)–C(9)	109 (1)	N(5)–C(9)–C(8)	112 (1)
N(6)–C(10)–C(11)	117 (1)	C(10)–C(11)–C(12)	118
C(10)–C(11)–C(16)	119	C(12)–C(11)–C(16)	120
C(11)–C(12)–C(13)	120	C(11)–C(12)–C(17)	123 (1)
C(13)–C(12)–C(17)	116 (1)	C(12)–C(13)–C(14)	120
C(12)–C(13)–C(18)	122 (1)	C(14)–C(13)–C(18)	118 (1)
C(13)–C(14)–C(15)	120	C(13)–C(14)–C(21)	118 (1)
C(15)–C(14)–C(21)	120 (1)	C(14)–C(15)–C(16)	120
C(14)–C(15)–C(19)	119 (1)	C(16)–C(15)–C(19)	121 (1)
C(11)–C(16)–C(15)	120	C(11)–C(16)–C(20)	120 (1)
C(15)–C(16)–C(20)	119 (1)	N(7)–C(21)–C(14)	117 (1)
N(7)–C(22)–C(23)	112 (1)	N(8)–C(23)–C(22)	113 (1)
N(8)–C(24)–C(25)	110 (1)	N(7)–C(25)–C(24)	110 (1)
N(8)–C(26)–C(27)	123 (1)	N(8)–C(26)–C(37)	115 (1)
C(27)–C(26)–C(37)	121 (1)	C(26)–C(27)–C(28)	120 (1)
C(26)–C(27)–C(29)	124 (1)	C(28)–C(27)–C(29)	114 (1)
N(2)–C(28)–C(27)	124 (1)	N(3)–C(29)–C(27)	121 (1)
N(3)–C(29)–C(30)	120 (1)	C(27)–C(29)–C(30)	119 (1)
N(3)–C(31)–C(32)	111 (1)	C(31)–C(32)–C(33)	115 (1)
N(4)–C(33)–C(32)	110 (1)	N(2)–C(34)–C(35)	110 (1)
C(34)–C(35)–C(36)	113 (1)	N(1)–C(36)–C(35)	111 (1)
C(26)–C(37)–C(38)	115 (1)	C(37)–C(38)–C(391)	122 (1)
C(37)–C(38)–C(392)	128 (2)	C(38)–C(391)–C(40)	114 (2)
C(38)–C(392)–C(40)	119 (3)	C(391)–C(40)–C(41)	109 (2)
C(392)–C(40)–C(41)	137 (2)	C(40)–C(41)–C(421)	135 (2)
C(40)–C(41)–C(422)	107 (2)	C(41)–C(421)–C(431)	108 (2)
C(41)–C(422)–C(431)	136 (2)	C(41)–C(421)–C(432)	129 (2)
C(41)–C(422)–C(432)	113 (2)	C(421)–C(431)–C(44)	113 (2)
C(422)–C(432)–C(44)	115 (2)	C(5)–C(44)–C(432)	113 (2)
C(5)–C(44)–C(431)	112 (1)		
	(c) Solvent Acetonitrile		
N(51)–C(51)–C(52)	165 (2)		

transfer it to the alternate metal ion. In common with the complexes studied earlier[15,16] the nickel(II) ion is readily removed from the typical R^3-bridged complexes (structure V) by reaction with HCl gas. This provides the route to the synthesis of the complexes of such potentially reactive ions as cobalt(II) and iron(II). In contrast, attempts to remove the tricyclic ligands (structure VI) from nickel(II) and transfer them to other metal ions have failed. Although products appearing to be ligand salts are generated by removal of nickel(II) from the parent complex, pure products have not been obtained from the subsequent attempts to synthesize cobalt(II) and iron(II) derivatives. Indeed, the ligand salts will not even react with nickel(II) to regenerate the starting materials. Either the doubly bridged ligand salts are unstable under the conditions used to isolate them or they undergo some rearrangement that inhibits the subsequent coordination to a metal ion.

Structure and Properties of a Doubly Bridged Vaulted Cyclidene Complex of Nickel(II). This unusual complex (structure VII, R^1 = 3,6-durylene, $R^3 = (CH_2)_8$) gives promise of good qualities as a host for the formation of inclusion complexes with small organic guest molecules such as alcohols. Earlier studies with the vaulted complexes have fully characterized their hydrophobically driven inclusion complexation with alcohols and phenols in aqueous solution.[7-9,18,19] The new host design has several additional advantages. Each of the bridging groups plays a distinctive role in moderating the binding of an included species while they act in concert to increase the fractional area of the void that is bounded by hydrophobic groups. The R^3 bridge will determine the dioxygen affinity of any cobalt(II) or iron(II) complex that can be prepared from the ligand, while the piperazine risers and durylene bridge define the general dimensions of the cavity available to a hydrophobically bound guest. As the X-ray structure shows (Figures 1 and 3), the R^3 bridging group closes the larger entry into the

(18) Kwik, W.-L.; Herron, N.; Takeuchi, K. J.; Busch, D. H. *J. Chem. Soc., Chem. Commun.* **1983**, 409.

(19) Meade, T. J.; Kwik, W.-L.; Herron, N.; Alcock, N.; Busch, D. H. *J. Am. Chem. Soc.* **1986**, *108*, 1954.

(20) Korybut-Daszkiewicz, B.; Kojima, M; Cameron, J. H.; Herron, N.; Chavan, M. Y.; Jircitano, A. J.; Coltrain, B. K.; Neer, G. L.; Alcock, N. W.; Busch, D. H. *Inorg. Chem.* **1984**, *23*, 903.

(21) *International Tables for X-ray Crystallography*; Kynoch: Birmingham, England, 1974; Vol. IV.

(22) Sheldrick, G. M. *SHELXTL User Manual*; Nicolet Instrument Co.; Madison, WI, 1981.

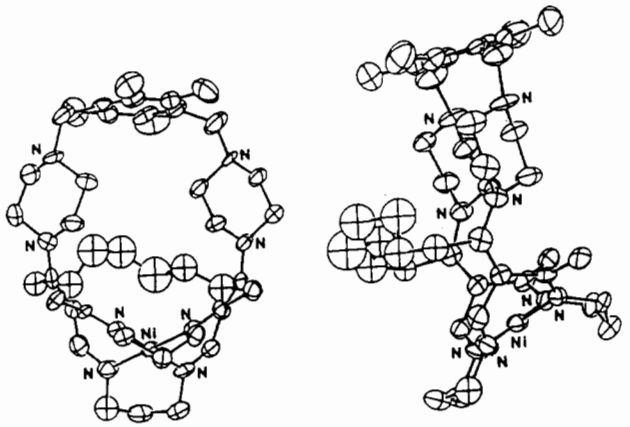

Figure 1. ORTEP drawings of the structure of $[Ni\{(CH_2)_8(CH_2pipz)_2$-(3,6-dur)[16]cyclidene$\}](PF_6)_2 \cdot CH_3CN$. Only one conformation of the polymethylene ring is shown for clarity.

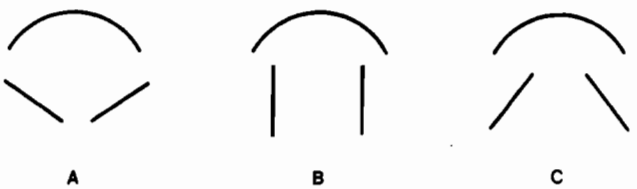

Figure 2. Sketch showing orientations of piperazine risers (straight-line segments) with respect to the polymethylene bridge (arc): (A) void closed; (B) void open; (C) void partially filled.

vault, effectively decreasing the area of the largest available opening through which a guest may enter the void.

The enhanced hydrophobic nature of the guest site is expected to produce a substantial increase in the equilibrium constant for the host–guest binding. Attempts to apply the same NMR techniques[7,9] to the new host that were used to characterize the first examples of vaulted cyclidene hosts have been unsuccessful. However, the results have been informative as well as disappointing. Takeuchi showed that solvent water molecules form hydrogen bonds to nitrogen atoms of the piperazine risers in vaulted cyclidene hosts (structures II and IV). Further, large ^{13}C chemical shifts (<0.5 ppm) occur for certain of the carbon atoms of the host upon inclusion of a guest because the water molecules are displaced from the cavity by the guest. The signs of these shifts are also unique for specific carbon atoms. In contrast, the new doubly bridged host (structure VII) shows only very small chemical shifts on the order of 0.2 ppm when guests are added to the solution. In addition, the shifts for all the carbons studied were of the same magnitude and sign. In view of the structure of this host it is suggested that its enhanced hydrophobic character prevents entry of water molecules into the cavity so that no hydrogen bonds are available for subsequent disruption when a guest enters the cavity. While this behavior supports the expected greater hydrophobic character of the cavity, it also denies us a powerful tool for the study of the corresponding inclusion complexes. Additional techniques are being developed in our laboratories for the study of this promising new kind of host. Our inability to obtain the free ligand and transfer it to other metal ions is a more limiting obstacle to the continuing study of the doubly bridged, vaulted host. Attempts are under way to use other templating metal ions in these syntheses in order to either produce iron(II), cobalt(II), and/or copper(II) complexes, which are of immediate interest, or provide a successful route to the free ligand. The X-ray crystal structure determination reported here provides substantial insight into the probable chemistry of this unique host species and removes all doubt as to its identity. NMR data are available as supplementary material.

The results of the X-ray determination of the structure (VII) of $[Ni\{(CH_2)_8(CH_2pipz)_2(3,6\text{-dur})[16]cyclidene\}](PF_6)_2 \cdot CH_3CN$ (pipz = piperazine, dur = durylene) confirm our success in creating a large hydrophobic cavity surrounding one axial coordination site of the metal. As shown in Figure 1, the durylene bridge

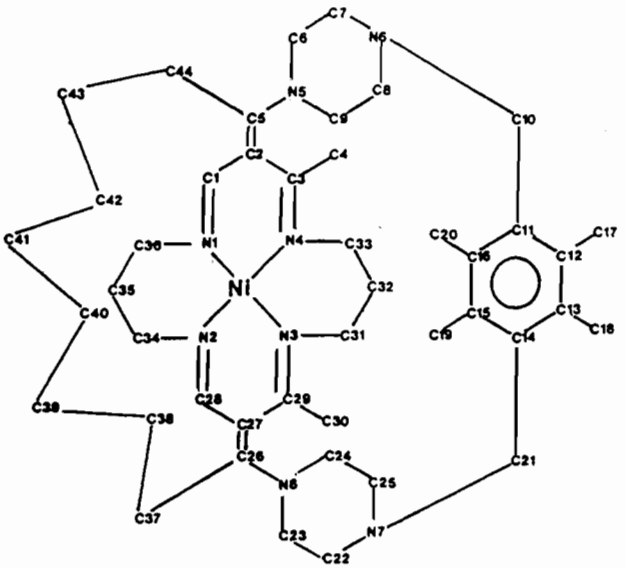

Figure 3. Numbering scheme for $[Ni\{(CH_2)_8(CH_2pipz)_2(3,6\text{-dur})[16]$-cyclidene$\}](PF_6)_2 \cdot CH_3CN$.

Scheme III

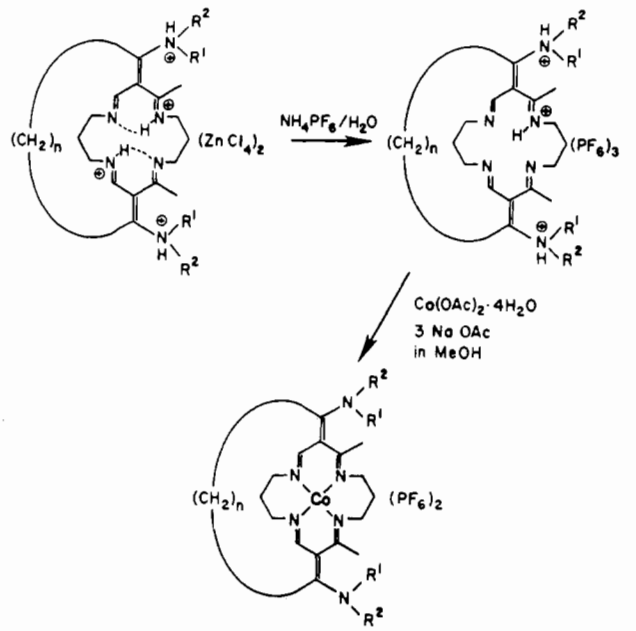

effectively forms a roof to the void with the piperazine units forming the sides. The piperazine units adopt chair conformations and are twisted inward toward the void. The cyclidene macrocycle adopts the typical saddle conformation with the saturated trimethylene chelate rings being on one side of the Ni–4N plane and the unsaturated, substituted chelate rings on the opposite. Most importantly, the polymethylene bridge is shown to cap one side of the void and effectively leaves only one side of the void completely open to approach by solvent or substrate molecules. This structural arrangement should definitely increase the hydrophobicity of the cavity by closing off one side of the void to approach by solvent molecules. Furthermore, in the observed solid-state conformation, the twist of the piperazine rings effectively blocks the other side. This is shown in sketch A in Figure 2. These sketches show the alignments of the piperazine and the retro-bridge as viewed from the roof (durylene group) of the structure. The retro-bridging chain is represented by the arc, and the two piperazine risers, by straight line segments. In A, the canting of the piperazines makes them part of an almost continuous wall encompassing the void within the complex. Although the rotation of the piperazine groups (to form orientations B and C) is presumably fairly facile, the conformation favored in solution may

Table VIII. Analytical Data for Cobalt(II) Complexes (Structure V) of the R^3-Bridged Ligands (PF_6^- Salts)

			anal., %							
			calcd				obsd			
n^a	R^2	R^1	C	H	N	Co	C	H	N	Co
5[b]	Me	Me	39.71	5.55	12.01	7.22	39.81	5.65	12.04	7.10
6[b]	Me	Me	40.49	5.70	11.80	7.09	40.26	5.69	11.47	7.18
7[c]	H	Me	40.01	5.60	10.37	7.27	39.81	5.34	10.77	7.24
7[d]	Me	Me	39.47	5.89	10.23	7.17	39.40	6.04	9.97	6.81
7[b]	H	*n*-Pr	42.67	6.12	11.24	6.75	42.58	5.85	11.16	6.64
8[b]	Me	Me	41.96	5.99	11.42	6.86	42.09	6.04	11.45	6.80

[a] For the $(CH_2)_n$ bridge. [b] Contains 1 mol of MeCN. [c] Contains $^1/_2$ mol of C_2H_5OH. [d] Contains 1 mol of H_2O.

Table IX. Electrochemical Data for R^3-Bridged Complexes of Cobalt(II) and Iron(II)[a] (Structure V)

			oxidn				redn			
R^3	R^2	R^1	$E_{1/2}$, V	Δ_1, mV	E_p, V	Δ_2, mV	$E_{1/2}$, V	Δ_1, mV	E_p, V	Δ_2, mV
					(a) Cobalt Complexes					
$(CH_2)_5$	CH_3	CH_3	0.19	70	0.23	70	*d*		−1.62[c]	
			0.82	70	0.85	60	*d*		−1.73	
							d		−2.27	
							d		−2.42	
$(CH_2)_6$	CH_3	CH_3	0.19	100	0.22	80	*d*		−1.64[c]	
			0.80	70	0.82	60	*d*		−1.76	
							d		−2.34	
							d		−2.46	
$(CH_2)_7$	CH_3	CH_3	0.29[f]	70	0.33	70	−1.66	80	−1.66	80
			0.55	80						
			0.86	70	0.89	60			−2.48[d]	
			1.15	70						
$(CH_2)_8$	CH_3	CH_3	*b*		0.32[e]		−1.65	60	−1.61	60
					0.47					
					0.87	70				
					1.15[e]					
					1.31					
$(CH_2)_7$	CH_3	H	0.29	80	0.33	80			−1.66	
			1.20	90	1.22	70	*b*		−1.78	
							−2.17	80	−2.16	
$(CH_2)_7$	*n*-Pr	H	0.34	80	0.36	70	−1.63		−1.66	
			1.24	70	1.24	70			−1.82	
							−2.23		−2.17	
					(b) Iron Complexes					
$(CH_2)_7$	CH_3	CH_3	−0.48	90	−0.44		−2.12	210	−2.14	
			0.80		0.83					
			1.0							
$(CH_2)_8$	CH_3	CH_3	−0.40		−0.34		−2.2		−2.2	
			0.80		0.83				−2.45	
			0.98		1.01				−2.66	

[a] Conditions: in CH_3CN solution, 0.1 N *n*-Bu_4NBF_4 supporting electrolyte, $Ag/AgNO_3$ reference electrode (0.1 M). [b] RPE waves too close for accurate determination. [c] Shoulder on next peak. [d] Poor RPE waves. [e] Shoulder; RPE waves too close to be analyzed. [f] In stationary-electrode CV a reduction shoulder appears at 0.25 V followed by a sharp peak at 0.15 V.

well increase the difficulty of access to the void, in accord with the NMR observations reported above.

The dimensions of the cavity are quite similar to those reported for the vaulted complex (structures II and IV) [Ni{Me_2-(CH_2pipz)(9,10-anthra)[16]cyclidene}](PF_6)$_2$(anthra = anthracene).[8,9] The height of the cavity from the NiN_4 plane to the plane of the durylene ring (C11–C16, see Figure 3) is 8.3 Å. The cavity depth from a plane bisecting the four central atoms (C39–C42) of the methylene bridge to the methyl group on the cyclidene portion of the macrocycle (C4 and C30) is 6.0 Å, and the width from the nitrogen atoms of one piperazine unit (N7 and N8) to a plane bisecting the second piperazine unit is 4.6 Å. The cavity height is larger than the 5.4 Å reported for the lacunar complex [Ni{$(C_6H_5)_2(NCH_2C_6H_5)_2$(*m*-xyl)[16]cyclidene}](PF_6)$_2$ (xyl = xylyl; structures I and III) but is similar to the 8.5-Å value reported for the vaulted complex [Ni{$Me_2(CH_2pipz)_2$(9,10-anthra[16]-cyclidene}](PF_6)$_2$ (structures II and IV).[7,8] Although larger cavity sizes would be desirable for some of the larger substrates, this cavity should be quite appropriate for such substrates as butanol and some substituted benzenes.

A particularly distinctive feature of this complex is associated with the presence of the second bridging group. As our studies with the dioxygen complexes of iron(II) and cobalt(II) show (vide infra), the retro-bridge places steric constraints on the axial binding site inside the void. This should favor the coordination of large ligands at the external site and help maintain the five-coordinate structure in the absence of dioxygen and similar small ligands. This is obviously important since a ternary complex of the desired kind (metal chelate–substrate–dioxygen) requires a vacant binding site inside the void that can be used for dioxygen binding. Thus, the bridging group constituted by the piperazine risers and the durylene group provides a large cavity for guest, or substrate, binding, while the shorter polymethylene retro-bridge segments the cavity, producing a more confined region within which dioxygen affinity may be controlled.

Synthesis and Characterization of the Cobalt(II) Complexes. The synthetic route to the cobalt(II) complexes of the macrobicyclic, R^3-bridged ligands (structure V) is outlined in Scheme III. The ligand salt obtained by removal of nickel(II) from the parent complex is first metathesized to the PF_6^- salt. This procedure gives a ligand salt that is free of zinc ion. This is necessary because zinc(II) competes with the cobalt(II) for the coordination site within the cyclidene ligand.

For ligands of structure V, those having only one bridging group

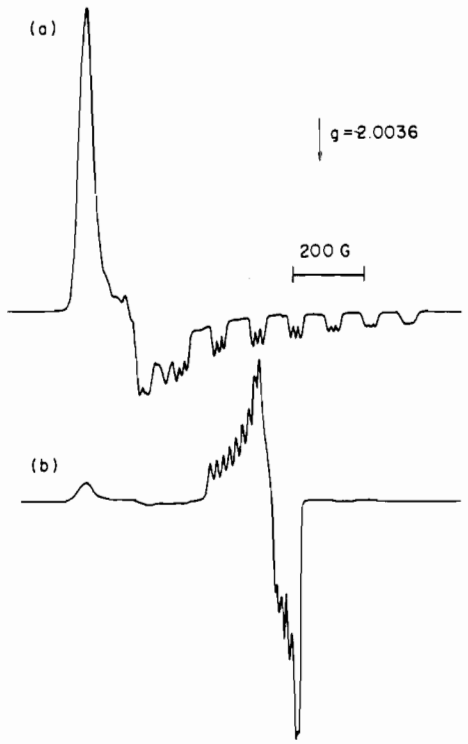

Figure 4. ESR spectra in acetone solution at −196 °C of the square-pyramidal cobalt(II) complexes of retro-bridged cyclidene ligands and their dioxygen adducts: (a) [Co{$(CH_2)_8(NMe_2)_2Me_2$[16]cyclidene}(Mim)]$(PF_6)_2$; (b) [Co{$(CH_2)_8(NMe_2)_2Me_2$[16]cyclidene}(Mim)(O_2)]$(PF_6)_2$.

(R^3), the cobalt(II) complexes are readily prepared. Analytical data for the complexes are presented in Table VIII and electrochemical data in Table IX. For the complexes with $R^1 = R^2 =$ Me and $R^3 = (CH_2)_5$ or $(CH_2)_6$, the Co^{II}/Co^{III} half-wave potential occurs at 0.19 V. With the longer bridges, $R^3 = (CH_2)_7$ or $(CH_2)_8$, the potential shifts slightly to about 0.30 V. The dependence of the half-wave potential on bridge length is a complex subject that has been treated at length elsewhere for the R^1-bridged cobalt(II) complexes (structures I and III).[23] The limited data available for the R^3-bridged species do not merit similar attention. For the two complexes with heptamethylene bridging groups and R^1 = H and R^2 = Me or *n*-Pr, the Co^{II}/Co^{III} potential is 0.29 and 0.34 V, respectively. These values are very close to those of the corresponding complexes having R^1 = Me. This very slight change is surprising in view of the larger effect observed among nickel(II) complexes with the same ligands.

Dioxygen Adducts of the R^3-Bridged Cobalt(II) Complexes. Surprisingly, the affinities of the cobalt complexes of R^3-bridged ligands (structure V) for dioxygen are much lower than those of the related R^1-bridged complexes (structures I and III). Electronic and ESR spectra were used to study the O_2 adducts of the six cobalt(II) complexes having structure V in acetonitrile solutions containing 1.5 M 1-methylimidazole (MIm). These conditions maximize the dioxygen affinities of the complexes, and since MIm coordinates to the unhindered side of the molecule, it prevents the binding of dioxygen to that open site. Thus the strongly bound axial ligand prevents the deleterious dimerization process that is often observed in cobalt(II)–dioxygen systems.[24,25] Earlier studies on R^1-bridged cobalt(II) complexes produced values of K_B, the equilibrium constant for coordination of the axial base 1-methylimidazole (eq 1), of about 10^2 and indicated that >99% of the cobalt(II) exists in the five-coordinate form under these conditions.[11]

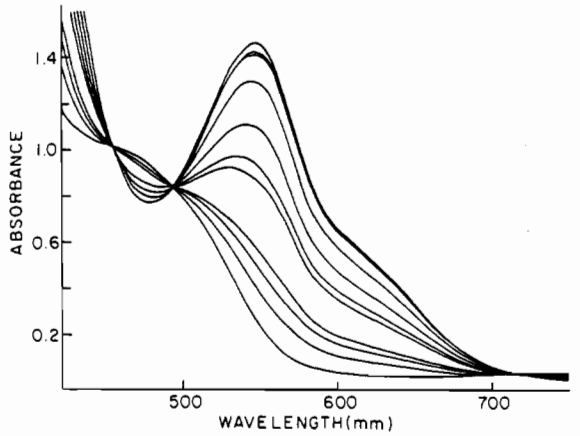

Figure 5. Electronic spectra of an acetone solution of [Fe{$(CH_2)_8(NMe_2)_2Me_2$[16]cyclidene}Cl](PF_6) at different partial pressures of O_2 at −41.0 °C. Partial pressures: ~0, 0.2, 1.1, 1.9, 4.6, 6.2, 17, 38, 99, 150, 760 torr.

Table X. ESR Parameters[a] for Square-Pyramidal, Low-Spin Cobalt(II) Complexes of the R^3-Bridged Ligands (Structure V) and Their Dioxygen Adducts

R^2	R^3	$g_\perp$	$g_\parallel$	$A_\parallel$, G	$A_\perp$, G
		Cobalt(II) Complexes			
CH_3	$(CH_2)_5$	2.311	2.015	102	15
CH_3	$(CH_2)_6$	2.316	2.014		
CH_3	$(CH_2)_7$	2.319	2.009	104	15
CH_3	$(CH_2)_8$	2.286	2.007	100	13
H	$(CH_2)_7$	2.286	2.006	102	13
H	$(CH_2)_7$	2.286	2.008	100	15
		Dioxygen Adducts			
CH_3	$(CH_2)_7$	2.014	2.081	18	8
CH_3	$(CH_2)_8$	2.010	2.086	18	10
H	$(CH_2)_7$	2.012	2.078	18	10
CH_3	$(CH_2)_7$	2.014	2.085	18	9

[a] Estimated standard deviations: $g_\perp$ and $g_\parallel$ ±0.002; $A_\perp$ and $A_\parallel$, ±0.56 G. Conditions: acetone solvent, 1-methylimidazole axial base, frozen glass at −196 °C. R^1 in all cases is $(CH_3)_2$.

$$[Co(L)]^{2+} + B \rightleftharpoons[K_B] [Co(L)B]^{2+} \quad (1)$$

The ESR spectra of the unoxygenated form of the retro-bridged cobalt(II) complexes (structure V) confirm the five-coordinate nature of the species in solution (Figure 4a, Table X). All ESR spectra are typical of square-pyramidal, low-spin cobalt(II) complexes,[24,25] displaying axial patterns with $g_\perp \cong 2.3$ and $g_\parallel \cong 2.0$. The parallel component is split into eight bands from coupling with ^{59}Co ($I = {}^7/_2$), and each of the eight bands is split into an equal-intensity triplet by the interaction of the unpaired electron with the ^{14}N atom ($I = 1$) of the single axial MIm.

On exposure of the solutions to dioxygen, ESR spectral patterns characteristic of the 1:1 dioxygen adducts are observed (Figure 4b, Table X), with $g_1 \cong g_2 \cong 2.01$ and $g_3 \cong 2.08$. Typically, both parallel and perpendicular components display hyperfine splitting, but the coupling constants for the parallel component are at least a factor of 5 smaller than those of the oxygen-free compound. The difference in ESR spectra from compound to compound and among their dioxygen adducts are generally very slight. The most striking differences occur among the spectra of the dioxygen adducts, and they reflect different extents of dioxygen adduct formation under identical conditions.

On this basis it is apparent that the dioxygen affinity increases from R^3 = pentamethylene to octamethylene. From Table VIII, both the half-wave potentials and the peak potentials for the complexes shift to more positive values in this sequence. Since the cobalt(II) complexes become more difficult to oxidize as the bridge length increases, the enhanced dioxygen affinities are not derived from increased electron density on the cobalt. We therefore conclude that the enhanced dioxygen affinity arises from

(23) (a) Chavan, M. Y. Ph.d. Dissertation, The Ohio State University, 1983. (b) Chavan, M. Y.; Meade, T. J.; Busch, D. H.; Kuwana, T. *Inorg. Chem.* **1986**, *25*, 314.
(24) Jones, R. D.; Summerville, D. A.; Basolo, F. *Chem. Rev.* **1979**, *79*, 139.
(25) Niederhoffer, E. C.; Timmons, J. H.; Martell, A. E. *Chem. Rev.* **1984**, *84*, 137.

Table XI. Oxygen Binding Constants[a] for Dioxygen Adducts of the R^3-Bridged Cobalt(II) Complexes (Structure V)

n[b]	R^2	R^1	T, °C	K_{O_2}, $torr^{-1}$
7	H	Me	0.0	0.0020 ± 0.0001[c]
			−10.0	0.0047 ± 0.0003
			−14.4	0.0081 ± 0.0005
			−20.2	0.015 ± 0.001
7	H	*n*-Pr	0.0	irrev
			−14.8	0.014 ± 0.001
8	Me	Me	−25.0	0.0037 ± 0.0002
			−33.2	0.0099 ± 0.0003
			−37.6	0.020 ± 0.001

[a] Measured in CH_3CN solution containing 1.5 M 1-methylimidazole. [b] For the $(CH_2)_n$ bridge. [c] Not completely reversible.

steric effects associated with the change in bridge length. This provides an unambiguous and uncomplicated demonstration of the steric source of the control of dioxygen affinity by lacunar bridging groups. Earlier examples, involving R^1-bridged lacunar cyclidene complexes of cobalt(II) (structures I and III), were less clear in this regard because the increase in dioxygen affinity paralleled both a shift toward negative potentials and an increase in the length of the bridging groups.[23]

Precise determinations of equilibrium constants for dioxygen binding (K_{O_2}) were carried out on three of the new complexes having structure V (eq 2). The values were determined by

$$[Co(L)B]^{2+} + O_2 \rightleftarrows [Co(L)B(O_2)]^{2+} \qquad (2)$$

electronic spectroscopy, as reported earlier,[11] and the results are listed in Table XI. The effect exerted by the bridge is clearly evident in the values of K_{O_2}. For structure V with $R^3 = (CH_2)_8$ and $R^2 = R^1 = Me$, the value of K_{O_2} at −24.0 °C is 0.0037 $torr^{-1}$ while the value for the related heptamethylene-bridged complex is too small to measure by our techniques (<0.0005 $torr^{-1}$). Shortening the chain length by only one methylene unit has a profound effect on the ability of the complex to bind dioxygen.

Another large effect is associated with the replacement of one methyl group of the $-N(CH_3)_2$ moiety with a hydrogen atom. Despite the short bridge length, the heptamethylene-bridged "N–H" compound has a binding constant that is a factor of 6 greater than that for the octamethylene "N–methyl" compound, when the values are extrapolated to the same temperature. Not only does the change in bridge length lead one to expect the opposite result, but the values of the electrochemical parameters for the two complexes (Table IX) are almost identical so that bridge length would be expected to be the dominant factor in determining dioxygen affinity.

A number of possibilities must be considered in attempting to explain this rather large effect. Since increased polarity of environment is known to enhance dioxygen affinity among cobalt–dioxygen carriers,[11b] one might expect that the presence of the relatively polar N–H group in place of an N–Me group could be responsible for the increase in dioxygen affinity. This is obviated by the fact that no such effect is seen among the dioxygen adducts of the R^1-bridged cyclidene complexes of cobalt(II) (structures I and III). Similarly, we can discard a second possible source of the larger dioxygen affinity of the N–H derivative: steric interference between substituents on the $-NR_2$ group and the bound dioxygen. With use of R^1-bridged complexes of both cobalt(II) and iron(II) (structures I and III), the effect of these substituents has been studied extensively, as have steric interactions with bound dioxygen, and it has been shown that substituents at this position do not interact sterically with the coordinated O_2.

The remaining possibility arises from orientational effects associated with the planarity of the $-NR_2$ group.[14-17,26] Structures IX and X show the so-called *lid-on* and *lid-off* isomers of the lacunar complexes; they also show the positions of R^3 and R^4 (always a methyl group). When R^1 (the bridge in those earlier studies, structure I) is in the more vertical position, the structure is identified as lid-on. Obviously, placement of the bridge group

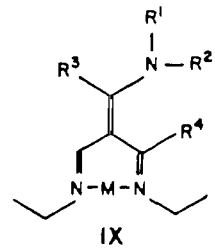

IX

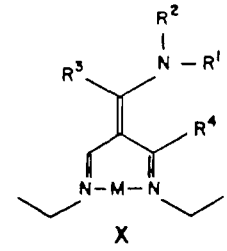

X

in the horizontal position gives the lid-off isomer. When this bridge nitrogen is tertiary, the R^1-bridged complexes tend to place the more bulky group in the lid-off position. Thus, when R^1 is a *m*-xylylene bridge and R^2 is methyl, the lid-off isomer occurs.[15,16] This suggests that the steric repulsion between R^3 and a bulky R^1 group is more difficult to accommodate than other repulsions, such as that between R^1 and R^4. This is consistent with the supposition that the second N–Me group forces the octamethylene bridge into a constrained conformation that crowds the bound dioxygen and lowers the dioxygen affinity.

The magnitudes of these binding constants for complexes having structure V are much lower than those for the corresponding R^1-bridged cobalt(II) complexes of structure I. For example, the complex I with $R^1 = (CH_2)_6$ and $R^2 = R^3 = Me$, which has an eight-membered bridge containing two nitrogen atoms, has K_{O_2} = 4.6 $torr^{-1}$, a value that is $\sim 10^4$ greater than K_{O_2} for the complex V having an eight-membered bridging group and $R^2 = R^1 = Me$. This difference must arise either from the contrasting geometry of the bridge nitrogen atom, in the first case, and from the carbon atom that replaces it in the second, or from a novel polar effect related to the difference of 180° in the orientation of the angular Co–O–O unit. The almost planar bridge-nitrogen atoms in structure I appear to provide more space for the bound dioxygen molecule than do the tetrahedral carbons in structure V. For complexes of the latter type, molecular models suggest that the bridge must lie much closer to the metal and more directly over the center of the coordination plane of the metal ion. This may produce a more geometrically constrained pocket and, consequently, diminished dioxygen affinities as compared to those of complexes of structure I. The polar bridge nitrogen is closest to the more distant (from Co) oxygen atom in the R^3-bridged complex, and this might seem to favor an enhanced dioxygen affinity for these species, the reverse of our observations. Thus the geometric factor seems to dominate.

For the heptamethylene R^3-bridged lacunar cobalt(II) complex with $R^2 = Me$ and $R^1 = H$ (structure V), equilibrium constant data were collected over a sufficiently wide temperature range to permit the estimation of thermal parameters (ΔH = 13.8 ± 0.6 kcal mol^{-1}; ΔS = −62 ± 2 eu; standard state of 1 torr) and these are similar to the parameters calculated for dioxygen adduct formation under similar conditions by several complexes of structure I.[10] The values of ΔH fall in the range −14 to −18 kcal mol^{-1}, and the ΔS values are the same, within experimental error, for all of the cases that have been studied, −65 ± 3 eu. The lower values for ΔH are found for complexes that have shorter bridge lengths, and it is concluded that the weakened interaction between cobalt(II) and dioxygen has an enthalpic source. The fact that the ΔH value for the R^3-bridged complex lies at the extreme low energy of the range reflects the steric demands of the heptamethylene bridging unit. The constancy of the entropy of the reaction suggests that the nature of the bridge has little effect on the ordering of the system. The entropy of gaseous molecular dioxygen is 62 eu (standard state of 1 torr[27], and the major contribution to the entropy of the reaction of dioxygen with the cobalt(II) complexes clearly derives from the loss of degrees of freedom of the dioxygen molecule on coordination.

Synthesis and Characterization of R^3-Bridged Iron(II) Complexes. The iron(II) complexes with cyclidene ligands are prepared by the reaction of the appropriate ligand salt with $Fe(CH_3CN)_2Cl_2$

(26) Herron, N.; Nosco, D. L.; Busch, D. H. *Inorg. Chem.* **1983**, *22*, 2970.

(27) *Handbook of Chemistry and Physics*, 53rd ed.; Weast, R. C., Ed.; Chemical Rubber Co.: Cleveland, OH, 1973; p D-55.

Table XII. Oxygen Binding Constants for R^3-Bridged Iron(II) Complexes (Structure V) in Acetone Solution

bridge	R^2	R^1	T, °C	K_{O_2}, torr^{-1}
$(CH_2)_8$	Me	Me	−41.0	0.219 ± 0.006[a]
			−34.9	0.118 ± 0.008
			−29.5	0.046 ± 0.004[a]
			−25.0	0.032 ± 0.002
			−20.7	0.019 ± 0.002
$(CH_2)_7$	Me	Me	−38.7	0.0055 ± 0.0001
			−28.1	dec

[a] Average of two determinations.

in acetonitrile. Two complexes have been prepared with ligands having structure V; the ligands contained the heptamethylene and octamethylene bridging groups, and both had methyl groups at the R^1 and R^2 positions. The compounds have been characterized by elemental analyses, and each has an axially coordinated chloride ligand and a PF_6^- counterion. Spectroscopic studies reveal that the chloride ion remains coordinated to the iron(II) ion in acetone solution, even in the presence of an excess of pyridine. A similar situation has been observed for an iron(II) complex of structure I,[12] where it was shown that the addition of water results in labilization of the chloride ion and formation of the pyridine derivative. Electrochemical data for the complexes are included in Table IX. The Fe^{III}/Fe^{II} couple for the heptamethylene derivative showed quasi-reversible behavior while that for the octamethylene species was irreversible. The potentials are typical for iron(II) cyclidene complexes having anionic axial ligands.[16]

Reaction of R^3-Bridged Lacunar Iron(II) Complexes with Dioxygen. In acetone solution, the complex of structure V having the octamethylene bridge forms a stable dioxygen adduct up to a temperature of −15 °C. At lower temperatures, the electronic spectra of the reaction mixture show sharply isosbestic behavior when recorded after equilibration with various partial pressures of dioxygen. This suggests that only two colored species are present in solution, the five-coordinate starting complex and the six-coordinate O_2 adduct, and attests to the reversibility of the oxygenation reaction. A typical set of such spectra is presented in Figure 5. The O_2 adduct exhibits an absorption maximum at 547 nm and a shoulder at 610 nm. Three isosbestic points occur at 454, 494, and 718 nm. The band maximum occurs at a wavelength that is 25 nm greater than that of the iron(II)–dioxygen complex of structure I.[12] The iron(II)–dioxygen adduct quantitatively dissociates upon flushing the system with N_2 gas.

Values of K_{O_2} are listed for various temperatures between −41.0 and −20.7 °C in Table XII. The equilibrium constant is 0.219 torr^{-1} at −41.0 °C, and this is much larger than that for R^1 = *m*-xylylene bridged lacunar complex having $R^2 = R^3$ = Me (structure I), for which K_{O_2} is 0.015 torr^{-1} (same axial ligand, temperature, solvent). The octamethylene-bridged complex of structure V has a much greater affinity for dioxygen. The thermodynamic parameters for the latter complex (ΔH = −14.5 ± 0.8 kcal mol^{-1}; ΔS = 65 ± 3 eu, standard state of 1 torr) show that the enthalpy of the reaction must account for the enhanced dioxygen affinity of this iron(II) complex. As expected, the entropy change is the same as observed for all lacunar dioxygen carriers. In view of the axial chloride ligand, it is perhaps surprising that this dioxygen carrier is not more susceptible to autoxidation.

The second R^3-bridged lacunar complex of iron(II), the heptamethylene-bridged species, has also been shown to undergo reversible oxygenation at low temperatures. The oxygen adduct has an electronic spectral absorption maximum at 552 nm and isosbestic points at 438, 560, and 698 nm. As anticipated for the shorter bridging group, the equilibrium constant for oxygenation is much smaller for this complex. At −39.7 °C in acetone solution, the chloro complex has an equilibrium constant of 0.0055 ± 0.0001 torr^{-1}, as compared with 0.166 torr^{-1} for the octamethylene-bridged complex (value obtained by extrapolation to this temperature). It should be noted that the complex with the shorter bridge is easier to oxidize by some 80 mV, a difference that leads to the prediction on electronic grounds that the dioxygen affinities would vary in the direction opposite to that observed. This reduction of K_{O_2} by a factor of 30 is dramatic testimony to the control of the dioxygen affinity by the bridge. At temperatures greater than about −30 °C, the complex undergoes rapid irreversible reaction with dioxygen. It is not clear why this species is so much more sensitive to autoxidation than its homologue. Evidence has been presented indicating that the autoxidation of lacunar complexes proceeds by an electron-transfer mechanism and that this autoxidation process is retarded by steric bulk surrounding the metal ion. On that basis one might speculate that the octamethylene group shelters the metal ion substantially more than does the heptamethylene group.

It has previously been found that the presence of a proton, rather than an alkyl group, at the R^2 position is accompanied by rapid autoxidation of the iron(II) dioxygen carriers with lacunar ligands.[16] Accordingly, incomplete studies on the iron(II) complex of the R^3-bridged ligand for which R^1 = Me, R^2 = H, and $R^3 = (CH_2)_7$ failed to show stable dioxygen adduct formation. Rapid irreversible decomposition occurs even at low temperatures.

Summary

By synthesizing lacunar and vaulted cyclidene complexes having bridging groups at the R^3 position (structure V), we have substantially extended the family of cyclidene complexes. The corresponding lacunar cobalt complexes are good dioxygen carriers but with dioxygen affinities several orders of magnitude lower than those of the analogous R^1-bridged species (structure I). These *retro-bridged* dioxygen carriers (structure V) unambiguously demonstrate the steric source of the dependence of dioxygen affinity on bridge length (for polymethylene bridges). The iron(II) dioxygen carriers (structure I) with these new ligands exhibit higher dioxygen affinities than the series of R^1 = *m*-xylylene bridged lacunar cyclidene iron(II) dioxygen carriers (structure I) reported earlier. While still requiring cooling for good reversible behavior, the examples studied are surprisingly insensitive to autoxidation. NMR data on the nickel(II) complexes support the earlier suggestion that bridge length may influence the π-orbital overlap that is responsible for impeding the rotation of the $-N(Me)_2$ substituents. Further, electrochemical studies show that this electronic interaction is not transmitted to the metal center.

Both lacunar and vaulted examples of a particularly attractive family of *doubly bridged* cyclidene complexes (structures VI and VII) have been synthesized and characterized. The crystal structure of the doubly bridged vaulted complex (structure VII) confirms the unusual structures of the series and shows that a well-defined cavity exists but that in the solid-state structure it is almost inaccessible. NMR studies suggest that this cavity is unusually hydrophobic for a cyclidene derivative, and we have not yet demonstrated the formation of inclusion complexes by this species. The failure of numerous attempts to remove the unaltered ligand from the templating nickel(II) ion have required the reformulation of both synthetic and physical chemical strategies.

Experimental Section

Physical Measurements. Electronic spectra were recorded on a Cary Model 17D spectrophotometer using 1-cm quartz cells. The values of the equilibrium constants for dioxygen adducts were determined by the procedure detailed in earlier reports.[11] ESR spectra were recorded on a Varian 102 spectrometer (DPPH reference). Microanalyses were performed by Galbraith Laboratories, Inc., Knoxville, TN. Carbon-13 NMR spectra were acquired with a Bruker WP80 spectrometer (20.115 MHz). Electrochemical measurements were performed as described previously.[15]

Structure Determination for [Ni{$(CH_2)_8(CH_2pipz)_2$(3,6-dur)[16]cyclidene}]$(PF_6)_2 \cdot CH_3CN$. Crystals suitable for X-ray analysis (yellow-green laths) were formed by slow evaporation of a 1:1 acetonitrile–ethanol solution of the complex. Crystal data are listed in Table IV. Preliminary measurements indicated orthorhombic symmetry with systematic absences $0kl$, $k + l$, and $h0l$, $h = 2n$, indicating space groups $Pna2_1$ or $Pnma$ (nonstandard setting of $Pnma$). The former was initially preferred as it seemed unlikely that the molecule contained a mirror plane, and this was shown to be correct by the successful refinement. Unit cell parameters and standard deviations were derived from a least-squares fit of 15 high-angle reflections. Data were collected with a Syntex $P2_1$ four-circle diffractometer. The θ–2θ technique was used with a variable

scan speed of 2.0–29° min^{-1}, depending on the intensity of a 2-s prescan. Backgrounds were measured at each end of the scan for one-fourth of the scan time. For the 45–50° shell, only reflections above a preset prescan count were measured. The scan range was ±1.0° around the $K\alpha_1$ to $K\alpha_2$ angles. Three standard reflections were measured every 200 reflections and showed slight changes during data collection. The data were scaled to correct for this. The data were corrected for Lorentz, polarization, and absorption effects (by the Gaussian method, using SHELXTL[22]). The maximum and minimum transmission factors for the latter were 0.92 and 0.86. Refinement was based on the 2709 reflections with $I/\sigma(I) \geq 2.5$.

The position of the nickel atom was obtained from a Patterson map, and subsequent Fourier syntheses revealed the location of the remaining non-hydrogen atoms. The z coordinate for Ni was held constant. One molecule of CH_3CN was revealed as solvent in the crystal. The carbon atoms of the durylene were held as a regular hexagon. Hydrogen atoms were given fixed isotropic temperature factors;[21] U = 0.07 Å. Those defined by the molecular geometry were inserted at calculated positions and not refined; methyl groups were treated as rigid CH_3 units, with their initial orientation taken from the strongest peak on a difference Fourier synthesis. The central atoms of the methylene chain (C39, C42, C43) were found to be disordered, having a major component with occupation factor 0.7 and a minor component with occupation factor 0.3. Final refinement was by cascaded least-squares methods. The largest peak on a final difference Fourier synthesis was of height 0.5 e $Å^{-3}$. A weighted scheme of the form $w = 1(\sigma^2(F) + gF^2)$ with g = 0.001 was used. The final R value was 0.055. This was shown to be satisfactory by a weight analysis. The chirality of the individual crystal was checked by refinement of a $\delta f''$ multiplier, which converged to +1. Computing was with the SHELXTL system[22] on a Data General NOVA3 computer. Scattering factors in the analytical form and anomalous dispersion factors were taken from ref 21. Final atomic coordinates are given in Table V and bond lengths and angles in Tables VI and VII.

Syntheses of the Nickel(II) Complexes. (3,11-Diacetyl-4,10-dimethyl-1,5,9,13-tetraazacyclohexadeca-1,3,9,11-tetraenato(2−)-κ^4N)nickel(II), [Ni(Ac_2Me_2[16]tetraenatoN_4)] (Scheme I, Starting Material). This complex was prepared by the previously published method.[28]

(2,12-Dimethyl-1,5,9,13-tetraazacyclohexadeca-1,4,9,12-tetraene-κ^4N)nickel(II) Hexafluorophosphate, [Ni(Me_2[16]tetraeneN_4)]$(PF_6)_2$ (Scheme I, First Product). This complex was synthesized by deacylation of [Ni(Ac_2Me_2[16]tetraenatoN_4)]. In a typical preparation 19.4 g (0.05 mol) of the starting complex and *p*-toluenesulfonic acid monohydrate (19.0 g; 0.1 mol) were refluxed for 5 min in 200 mL of methanol. The heat was removed, and a solution of NH_4PF_6 (18 g; 0.11 mol) in 50 mL of H_2O was added. The flask was cooled in a freezer, and the yellow crystals of product were collected, washed with methanol, and dried over P_2O_5 (yield 27.9 g, 93 %). The product was recrystallized from acetonitrile–ethanol. Anal. Found: C, 28.35; H, 4.17; N, 9.29; Ni, 9.63. Calcd for $C_{14}H_{24}N_4F_{12}NiP_2$: C, 28.17; H, 4.05; N, 9.38; Ni, 9.88.

(2,12-Dimethyl-1,5,9,13-tetraazacyclohexadeca-1,3,9,11-tetraenato-(2−)-κ^4N)nickel(II), [Ni(Me_2[16]tetraenatoN_4)] (Scheme I, Second Product). To a slurry of [Ni(Me_2[16]tetraeneN_4)]$(PF_6)_2$ (11.92 g; 0.02 mol) in 50 mL of methanol was added a solution of sodium methoxide (0.045 mol) in methanol. The base was prepared by reaction of Na metal (1.0 g) with 20 mL of methanol. The reaction mixture immediately became very dark purple. The solution was stirred for 5 min and then cooled in a freezer before the product was collected as a dark purple microcrystalline solid (yield 5.5 g, 90%).

(2,8-Diketo-10,16-dimethyl-11,15,18,22-tetraazabicyclo[7.7.7]tricosa-1(16),9(23),10,17-tetraenato(2−)-κ^4N)nickel(II), [Ni{$(CH_2)_5$(C=O)$_2Me_2$[16]tetraenatoN_4}], (2,9-Diketo-11,17-dimethyl-12,16,19,23-tetraazabicyclo[8.7.7]tetracosa-1(17),10(24),11,18-tetraenato(2−)-κ^4N)nickel(II), [Ni{$(CH_2)_6$(C=O)$_2Me_2$[16]tetraenatoN_4}], (2,10-Diketo-12,18-dimethyl-13,17,20,24-tetraazabicyclo[9.7.7]pentacosa-1(18),11-(25),12,19-tetraenato(2−)-κ^4N)nickel(II), [Ni{$(CH_2)_7$(C=O)$_2Me_2$[16]-tetraenatoN_4}], and (2,11-Diketo-13,19-dimethyl-14,18,21,25-tetraazabicyclo[10.7.7]hexacosa-1(19),12(26),13,20-tetraenato(2−)-κ^4N)nickel(II), [Ni{$(CH_2)_8$(C=O)$_2Me_2$[16]tetraenatoN_4}] (Scheme I, Third Product). These four complexes were prepared by the same procedure. The synthesis is described for [Ni{$(CH_2)_8$(C=O)$_2Me_2$[16]tetraenatoN_4}]. Two solutions, one containing [Ni(Me_2[16]tetraenatoN_4)] (3.05 g; 0.01 mol) and Et_3N (2.43 g; 0.024 mol) and the other sebacoyl chloride (2.39 g; 0.01 mol), each in 300 mL of ether, were simultaneously added to a vigorously stirred solution of 300 mL of ether, by use of a peristaltic pump. Addition was complete after ~3 h, and during this time an orange solid had appeared. The mixture was stirred for a further 30 min, and the solid material was collected by filtration. The solid was thoroughly washed with water to remove Et_3N·HCl. The remaining solid was dissolved in $CHCl_3$ and chromatographed on an alumina column, with $CHCl_3$ as the eluent. The orange-red band was collected, the solvent was removed, and the product was recrystallized from dichloromethane–ether (yield 3.0 g, 70%).

(2,8-Dimethoxy-10,16-dimethyl-11,15,18,22-tetraazabicyclo[7.7.7]tricosa-1,8,10,15,17,22-hexaene-κ^4N)nickel(II) Hexafluorophosphate, [Ni{$(CH_2)_5$(OMe)$_2Me_2$[16]cyclidene}]$(PF_6)_2$, (2,9-Dimethoxy-11,17-dimethyl-12,16,19,23-tetraazabicyclo[8.7.7]tetracosa-1,9,11,16,18,23-hexaene-κ^4N)nickel(II) Hexafluorophosphate, [Ni{$(CH_2)_6$(OMe)$_2Me_2$[16]-cyclidene}]$(PF_6)_2$, (2,10-Dimethoxy-12,18-dimethyl-13,17,20,24-tetraazabicyclo[9.7.7]pentacosa-1,10,12,17,19,24-hexaene-κ^4N)nickel(II) Hexafluorophosphate, [Ni{$(CH_2)_7$(OMe)$_2Me_2$[16]cyclidene}]$(PF_6)_2$, and (2,11-Dimethoxy-13,19-dimethyl-14,18,21,25-tetraazabicyclo[10.7.7]-hexacosa-1,11,13,18,20,25-hexaene-κ^4N)nickel(II) Hexafluorophosphate, [Ni{$(CH_2)_8$(OMe)$_2Me_2$[16]cyclidene}]$(PF_6)_2$ (Scheme II, First Product). These complexes were prepared by the same procedure. The synthesis of [Ni{$(CH_2)_8$(OMe)$_2Me_2$[16]cyclidene}]$(PF_6)_2$ is reported. To a solution of [Ni{$(CH_2)_8$(C=O)$_2Me_2$[16]tetraenatoN_4}] (5.5 g; 0.012 mol) in 300 mL of dried CH_2Cl_2 was added methyl fluorosulfonate (11.4 g; 0.1 mol) via a syringe. Over a period of 1 h, the red solution turned orange. The CH_2Cl_2 was removed, and the resultant orange oil was dissolved in EtOH (~200 mL). To this solution was added NH_4PF_6 (8.5 g; 0.05 mol) in EtOH, dropwise with stirring. The yellow solid was collected and recrystallized from acetonitrile–ethanol (yield 6.1 g, 66%). *Caution!* Methyl fluorosulfonate is a very toxic reagent.

(2,8-Bis(dimethylamino)-10,16-dimethyl-11,15,18,22-tetraazabicyclo-[7.7.7]tricosa-1,8,10,15,17,22-hexaene-κ^4N)nickel(II) Hexafluorophosphate, [Ni{$(CH_2)_5$(NMe_2)$_2Me_2$[16]cyclidene}]$(PF_6)_2$ (Structure V), (2,9-Bis(dimethylamino)-11,17-dimethyl-12,16,19,23-tetraazabicyclo-[8.7.7]tetracosa-1,9,11,16,18,23-hexaene-κ^4N)nickel(II) Hexafluorophosphate, [Ni{$(CH_2)_6$(NMe_2)$_2Me_2$[16]cyclidene}]$(PF_6)_2$ (Structure V), (2,10-Bis(dimethylamino)-12,18-dimethyl-13,17,20,24-tetraazabicyclo-[9.7.7]pentacosa-1,10,12,17,19,24-hexaene-κ^4N)nickel(II) Hexafluorophosphate, [Ni{$(CH_2)_7$(NMe_2)$_2Me_2$[16]cyclidene}]$(PF_6)_2$ (Structure V), and (2,11-Bis(dimethylamino)-13,19-dimethyl-14,18,21,25-tetraazabicyclo[10.7.7]hexacosa-1,11,13,18,20,25-hexaene-κ^4N)nickel(II) Hexafluorophosphate, [Ni{$(CH_2)_8$(NMe_2)$_2Me_2$[16]cyclidene}]$(PF_6)_2$ (Structure V). These four complexes were prepared by the same procedure. The synthesis of [Ni{$(CH_2)_8$(NMe_2)$_2Me_2$[16]cyclidene}]$(PF_6)_2$ is described. Dimethylamine gas was bubbled through a solution of [Ni{$(CH_2)_8$-(OMe)$_2Me_2$[16]cyclidene}]$(PF_6)_2$ (6.1 g, 7.7 mmol) in acetonitrile (200 mL). The solution changed immediately from yellow to dark red, and the flask became warm. Bubbling was stopped after 10 min and the flask was allowed to remain at room temperature for 1 day. The volume was then reduced to 10 mL, and the solution was passed down an alumina column, with acetonitrile as eluent. The volume was reduced and ethanol added to precipitate a yellow solid. The solid was recrystallized from acetonitrile–ethanol (yield 4.7 g; 75%).

(2,9-Bis(methylamino)-1,17-dimethyl-12,16,19,23-tetraazabicyclo-[8.7.7]tetracosa-1,9,11,16,18,23-hexaene-κ^4N)nickel(II) Hexafluorophosphate, [Ni{$(CH_2)_6$(NHMe)$_2Me_2$[16]cyclidene}]$(PF_6)_2$ (Structure V), (2,10-Bis(methylamino)-12,18-dimethyl-13,17,20,24-tetraazabicyclo-[9.7.7]pentacosa-1,10,12,17,19,24-hexaene-κ^4N)nickel(II) Hexafluorophosphate, [Ni{$(CH_2)_7$(NHMe)$_2$NMe_2[16]cyclidene}]$(PF_6)_2$ (Structure V), and (2,11-Bis(methylamino)-13,19-dimethyl-14,18,21,26-tetraazabicyclo[10.7.7]hexacosa-1,11,13,18,20,25-hexaene-κ^4N)nickel(II) Hexafluorophosphate, [Ni{$(CH_2)_8$(NHMe)$_2Me_2$[16]cyclidene}]$(PF_6)_2$ (Structure V). These three complexes were prepared in the same way as the dimethylamino derivatives except that methylamine gas was used instead of dimethylamine.

(2,10-Bis(*n*-propylamino)-12,18-dimethyl-13,17,20,24-tetraazabicyclo[9.7.7]pentacosa-1,10,12,17,19,24-hexaene-κ^4N)nickel(II) Hexafluorophosphate, [Ni{$(CH_2)_7$(NH-*n*-Pr)$_2Me_2$[16]cyclidene}]$(PF_6)_2$ (Structure V). To a solution of [Ni{$(CH_2)_7$(OMe)$_2Me_2$[16]cyclidene}]$(PF_6)_2$ (2.0 g; 2.57 mmol) in acetonitrile (100 mL) was added a solution of *n*-propylamine (0.45 g; 7.6 mmol) in 100 mL of acetonitrile. The solution changed from yellow to orange. After the solution was stirred for 10 h, the volume was reduced to 10 mL and the solution was passed down an alumina column. The fast-moving orange band was collected, the solution was reduced in volume, and ethanol was added to yield an orange microcrystalline solid (yield 1.6 g, 75%).

(13,19-Dimethyl-3,10,14,18,21,25-hexaazatricyclo[10.7.7.$6^{2,11}$]dotriaconta-1,11,13,18,20,25-hexaene-κ^4N)nickel(II) Hexafluorophosphate, [Ni{$(CH_2)_6$(NH)$_2$(CH_2)$_6Me_2$[16]cyclidene}]$(PF_6)_2$ (Structure VI), (13,19-Dimethyl-3,10,14,18,21,25-hexaazatricyclo[10.7.7.$7^{2,11}$]tritriaconta-1,11,13,18,20,25-hexaene-κ^4N)nickel(II) Hexafluorophosphate, [Ni{$(CH_2)_7$(NH)$_2$(CH_2)$_6Me_2$[16]cyclidene}]$(PF_6)_2$ (Structure VI), (13,19-Dimethyl-3,10,14,18,21,25-hexaazatricyclo[10.7.7.$8^{2,11}$]tetratriaconta-1,11,13,18,20,25-hexaene-κ^4N)nickel(II) Hexafluorophosphate, [Ni{$(CH_2)_8$(NH)$_2$(CH_2)$_6Me_2$[16]cyclidene}]$(PF_6)_2$ (Structure VI), (3,10,13,19-Tetramethyl-3,10,14,18,21,25-hexaazatricyclo[10.7.7.$6^{2,11}$]-

(28) Riley, D. P.; Busch, D. H. *Inorg. Synth.* **1978**, *18*, 36.

tetratriaconta-1,11,13,18,20,25-hexaene-κ^4N)nickel(II) Hexafluorophosphate, [Ni{$(CH_2)_8(NMe)_2(CH_2)_6Me_2$[16]cyclidene}]$(PF_6)_2$ (Structure VI), (14,20-Dimethyl-3,11,15,19,22,26-hexaazatricyclo[11.7.7.8^{1,12}]pentatriaconta-1,12,14,19,21,26-hexaene-κ^4N)nickel(II) Hexafluorophosphate, [Ni{$(CH_2)_8(NH)_2(CH_2)_7Me_2$[16]cyclidene}]$(PF_6)_2$ (Structure VI), (14,20-Dimethyl-3,11,15,19,22,26-hexaazatetracyclo-[11.7.7.7^{2,12}.1^{5,9}]pentatriaconta-1,5,7,9(28),12,14,19,21,26-nonaene-κ^4N)nickel(II) Hexafluorophosphate, [Ni{$(CH_2)_7(NH)_2(m$-xyl)Me_2-[16]cyclidene}]$(PF_6)_2$ (Structure VI), and (14,20-Dimethyl-3,11,15,19,22,26-hexaazatetracyclo[11.7.7.8^{2,12}.1^{5,9}]hexatriaconta-1,5,7,9(28),12,14,19,21,26-nonaene-κ^4N)nickel(II) Hexafluorophosphate, [Ni{$(CH_2)_8(NH)_2(m$-xyl)Me_2[16]cyclidene}]$(PF_6)_2$ (Structure VI). These seven complexes were prepared by very similar procedures. The synthesis is described for [Ni{$(CH_2)_8(NH)_2(CH_2)_7Me_2$[16]cyclidene}]$(PF_6)_2$. Two solutions, one containing [Ni{$(CH_2)_8(OMe)_2Me_2$[16]cyclidene}]$(PF_6)_2$ (1.58 g; 2.0 mmol) in acetonitrile (200 mL) and the other containing heptane-1,7-diamine (0.29 g; 2.2 mmol) in acetonitrile (200 mL) were added simultaneously, with use of a peristaltic pump, over a period of a few hours, to a vigorously stirred solution of acetonitrile (200 mL). The volume of the solution was reduced to 30 mL and the residual solution passed down an alumina column, with acetonitrile as eluent. The yellow band was collected, the solution was reduced in volume, and the product was precipitated by slow addition of methanol (yield 0.83 g, 48%).

Synthesis of Ligand Salts, $H_3L(PF_6)_3$. The PF_6^- salts of the various single-bridged ligands were prepared by the following procedure. The synthesis of [H_3[$(CH_2)_8(NMe)_2Me_2$[16]cyclidene]]$(PF_6)_3$ is described. Hydrogen chloride gas was bubbled through a solution of [Ni{$(CH_2)_8(NMe)_2Me_2$[16]cyclidene}]$(PF_6)_2$ (1.5 g; 1.84 mmol) in 50 mL of acetonitrile, and the solution rapidly changed from orange to green. After 10 min, bubbling was stopped and a solution of $ZnCl_4^{2-}$, prepared by reaction of Zn metal (0.75 g; 11.5 mmol) and HCl gas in acetonitrile, was added. A white solid precipitated and was collected and washed with acetonitrile. The solid was dissolved in water, and a solution of NH_4PF_6 (3.5 g; 21.5 mmol) in water was added dropwise with stirring to precipitate the product (yield 1.2 g, 72%).

Synthesis of Cobalt(II) Complexes. The complexes of the various singly bridged ligands were prepared by a single method. The synthesis of [Co{$(CH_2)_8(NMe)_2Me_2$[16]cyclidene}]$(PF_6)_2$ is described. A slurry of [H_3[$(CH_2)_8(NMe)_2Me_2$[16]cyclidene]]$(PF_6)_3$ (0.6 g; 0.66 mmol) in methanol (25 mL) was heated to reflux, and cobalt acetate tetrahydrate (0.18 g; 0.66 mmol) and sodium acetate (0.18 g; 1.98 mmol) in boiling methanol were added. The solution turned orange, and all of the solid dissolved. The mixture was refluxed for ~15 min. When the solution was cooled, orange crystals were formed (yield 0.35 g; 61%).

Synthesis of the Iron(II) Complexes. The two iron complexes were prepared by a common procedure. The synthesis is described for [Fe-{$(CH_2)_8(NMe)_2Me_2$[16]cyclidene}Cl](PF_6). A sample of the ligand salt [H_3[$(CH_2)_8(NMe)_2Me_2$[16]cyclidene]]$(PF_6)_3$ (0.51 g; 0.56 mmol) was dissolved in acetonitrile (20 mL), and $Fe(CH_3CN)_2Cl_2$ (0.12 g; 0.57 mmol) was added. To this solution was added Et_3N (0.24 g; 2.37 mmol), whereupon the yellow solution immediately turned deep red. The acetonitrile was removed by vacuum distillation to yield a red oil, which was dissolved in ethanol. A solution of NH_4PF_6 in ethanol was added to produce a deep red solid (0.26 g; 65%). The solid was recrystallized from acetonitrile–ethanol.

Acknowledgment. The support of the U.S. National Institutes of Health (Grant No. GM 10040) and of the U.S. National Science Foundation (Grant No. CHE-8402153) is greatly appreciated. FT-NMR spectra at 11.75 T (500 MHz) and 7.0 T (300 MHz) were obtained at The Ohio State University Chemical Instrument Center with equipment funded in part by NIH Grant No. 1 S10 RR01458-01A1. Travel support for the OSU/Warwick collaboration was provided by NATO.

Supplementary Material Available: Listings of NMR chemical shift values for host–guest complexing, X-ray thermal parameters, and H atom coordinates (4 pages); a table of calculated and observed structure factors (16 pages). Ordering information is given on any current masthead page.